

Model Order Reduction Techniques for Physics-Based Lithium-Ion Battery Management

A Survey

YANG LI, DULMINI KARUNATHILAKE,
D. MAHINDA VILATHGAMUWA,
YATEENDRA MISHRA, TROY W.
FARRELL, SAN SHING CHOI, and
CHANGFU ZOU

To unlock the promise of electrified transportation and smart grids, emerging advanced battery management systems (BMSs) will play an important role in the health-aware monitoring, diagnosis, and control of lithium-ion (Li-ion) batteries (see “Acronyms Used in This Article”). Sophisticated physics-based battery models incorporated into BMSs can offer valuable internal battery information to achieve improved operational safety, reliability, and efficiency and to extend the battery lifetimes. However, because they are developed from fundamental electrochemical and thermodynamic principles, rigorous physics-based models are saddled

with exceedingly high cognitive and computational complexity for practical applications.

This article reviews physics-based Li-ion battery model prevailing order reduction techniques to facilitate the development of next-generation BMSs. We analyze and comparatively characterize these procedures, mainly from the perspectives of model fidelity, computational efficiency, and application scope. By representing many effective and flexible reduced-order models (ROMs) as equivalent circuits, designers and practitioners who do not have electrochemical expertise but know circuit theory can gain insights into multiphysical dynamics as well as their coupling effects inside batteries. In addition,

ACRONYMS USED IN THIS ARTICLE

BMS:	battery management system
DAE:	differential algebraic equation
ECM:	equivalent circuit model
ESPM:	extended single particle model
EV:	electric vehicle
FDM:	finite-difference method
FVM:	finite-volume method
MOR:	model order reduction
HEV:	hybrid EV
P2D:	pseudo-2D
PDE:	partial differential equation
PDAE:	partial differential-algebraic equation
ROM:	reduced-order model
SEI:	solid-electrolyte interphase
SOC:	state of charge
SOH:	state of health
SPM:	single particle model
ODE:	ordinary differential equation

recommendations are made for selecting appropriate physics-based models for various applications in battery management. Finally, the prospect of physical model-enabled BMSs is discussed, including potential challenges and future research directions.

Introduction to Li-Ion Batteries and BMSs

Physics Behind Li-Ion Batteries

A typical Li-ion battery cell consists of many sandwich-like, thin layer structures, as depicted in Figure 1. It contains a porous positive electrode, a porous negative electrode, and a separator in between. The positive electrode contains various metal oxides or a mix of them, while the negative one is mostly graphite-based. In both, lithium species are assumed to be stored in the lattice sites of the solid phase particles. The separator is an electronic insulator that allows lithium ions to pass. The electrodes and the separator are immersed in a concentrated solution of charged lithium ions named the *electrolyte* [1].

During charging, the lithium species in the solid phase of the positive electrode diffuse to the surface of the

metal oxide particles, then react and transfer (de-intercalate) to the electrolyte as positively charged lithium ions. In the electrolyte, charged lithium ions travel toward the negative electrode by means of diffusion and migration. On the surface of the negative electrode, lithium ions react and intercalate into graphite particles. At the same time, the insulated separator forces electrons to flow in the opposite direction through the external electrical circuit connecting the current collector to a source. This de-intercalation/intercalation process is reversely applied when discharging to a load.

Apart from the intercalation/de-intercalation process, various side reactions occur in a cell, and most of them are detrimental to battery health. The major impact side reactions have on battery performance relates to lost storage capacity and increasing internal resistance, mainly caused by the growth of solid-electrolyte interphase (SEI) film and the deposition of metallic lithium, known colloquially as *lithium plating*. Side reactions occur most significantly at the separator/negative

electrode interface [2], and they consume the active materials in the electrodes in an irreversible way, leading to reductions in cyclable lithium species and charge/discharge rate capacity through time.

Vision of Advanced BMSs

It is essential for a BMS to accurately monitor internal battery states so that judicious operational strategies and reliable fault diagnosis can be performed [3]. Managing a Li-ion battery can slow cell aging, prevent cell failures, and avoid catastrophic fires/explosions due to unintentional overcharging/overdischarging, overtemperature, external and internal cell short circuits, and other stressed operating states. Indicators such as the state of charge (SOC) and state of health (SOH) are widely used in BMS algorithms to determine energy storage levels and battery degradation [4]. These states can also be used to derive information such as a battery's remaining useful energy and power capacity subject to operating limits placed on the terminal voltage, maximum current rate, and allowable

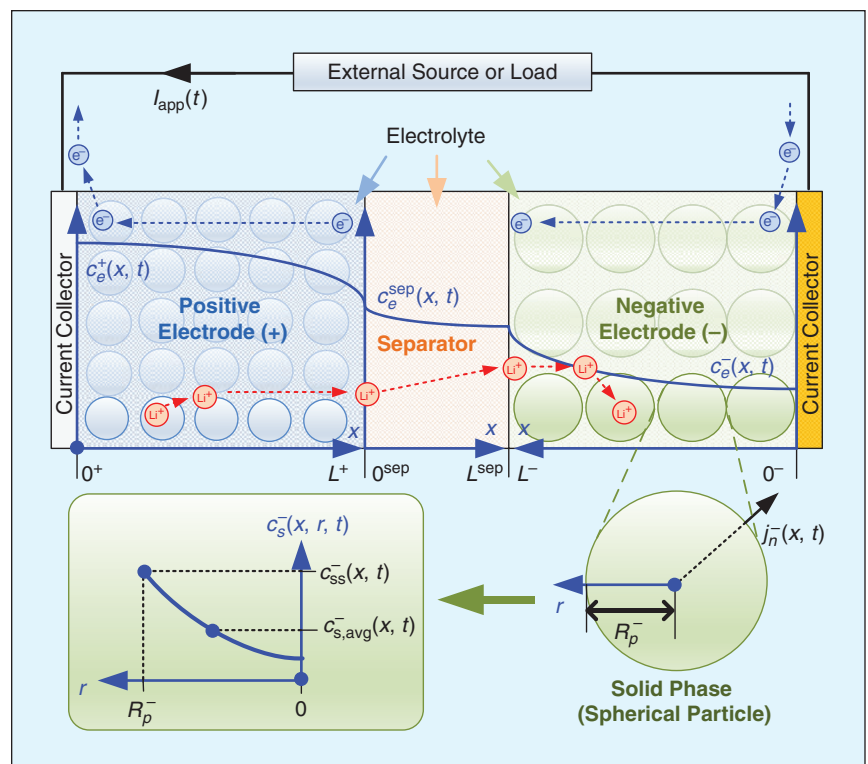


FIGURE 1 – The sandwich-like structure of a typical Li-ion battery cell during the charging process.

temperature range [5], [6]. In this way, battery capacity can be optimized to meet power control and energy management objectives [7], [8]. In addition, a BMS tracks variations in battery parameters through time, detects degradation, maintains cell balancing, and takes countermeasures to restrain the development of faults and prevent catastrophic failures so that battery life can be maximized [9].

However, none of the internal states and parameters can be directly measured: the battery terminal voltage, current, and surface temperature are the only quantities that are directly calculable through prevailing sensor technologies. Therefore, a suitable mathematical battery cell representation is often required in the design of model-based state/parameter estimators and control strategies [10], [11]. A battery model must be able to reproduce cell dynamics, with due consideration given to cell degradation, thermal effects, and parameter variations as environmental and operating conditions change. Also, a battery model should be sufficiently accurate to reflect nonlinearity and operating constraints, while computational efficiency and numerical stability should be guaranteed for real-time implementation to achieve control objectives [12].

Current Status of and Challenges to Conventional BMSs

Due to their mathematical simplicity, ease of implementation, and low-cost computation requirements, phenomenological equivalent circuit

models (ECMs) have been the most commonly used tools in the development of BMS algorithms [11], [13]. In an ECM, battery electrochemical dynamic behaviors are emulated by an electrical circuit consisting of basic components, such as capacitors, resistors, inductors, and controlled voltage/current sources. From the literature, a widely adopted ECM with n parallel RC branches is illustrated in Figure 2. Each circuit parameter, e.g., $R_0, C_0, R_1, C_1, \dots, R_n,$ and $C_n,$ is expressed as a function of battery SOC and temperature, and the identification of these functions requires a substantial number of offline tests and real-time tracking. Low-order, empirically based ECMs are affordable and well-suited to model batteries in applications that exhibit weak operating dynamics, e.g., supplying portable electronic devices, overnight electric vehicle (EV) charging, and renewable energy generation smoothing.

However, extrapolation beyond observed data is problematic for ECMs. BMSs for emerging applications, such as extremely fast EV charging, need to be designed for higher current rates, increased dynamic load requirements, and harsher operating environments. Under these circumstances, the model order, function complexity, and workload for tests to identify parameters have to be drastically increased to achieve high model accuracy. [14]. Furthermore, as circuit components do not bear direct relationships to electrochemical processes occurring in a battery, empirically based ECMs tend to convey limited information about

physically meaningful time-varying parameters, degradation mechanisms, and internal safety constraints. The estimation of battery performance becomes erroneous if evolving dynamic characteristics due to battery degradation are not properly taken into consideration. Furthermore, for the full exploitation of battery capability, ECMs are difficult to adapt to control algorithms with a predictive model due to a lack of insight into how future behaviors will be affected and about aging and safety levels [15]. In view of these reasons, commercial Li-ion battery systems are usually conservatively designed to facilitate the high uncertainty in predicting battery states and model parameters, increasing their size, weight, and cost.

First-Principle Model

To overcome problems with conventional ECMs and fully exploit the potential of Li-ion batteries, it is beneficial for a sophisticated health- and safety-aware battery management strategy to adopt physics-based models derived from fundamental electrochemical principles [14]. Based on the interpretation presented in the “Physics Behind Li-Ion Batteries” section, Doyle et al. introduced a basic multi-scale modeling framework for Li-ion batteries that is commonly referred to as the *pseudo-2D (P2D)* model or *Doyle-Fuller-Newman* model [16]–[18]. It consists of a set of partial differential algebraic equations (PDAEs) that describe the behaviors of several spatiotemporal variables, including the Li-ion concentration c_s and potential Φ_s in the solid phase of the electrode as well as the Li-ion concentration c_e and potential Φ_e in the electrolyte.

To uncover the common mathematical structure, the dynamic equations of the P2D model with 1D geometry can be generalized to the following partial differential equation (PDE) describing conservation laws:

$$M \frac{\partial u(z,t)}{\partial t} = \frac{1}{z^m} \frac{\partial}{\partial z} \left(z^m \delta \frac{\partial u(z,t)}{\partial z} \right) + \xi, \quad (1)$$

subject to the boundary conditions at $z = z_1$ and $z = z_2$:

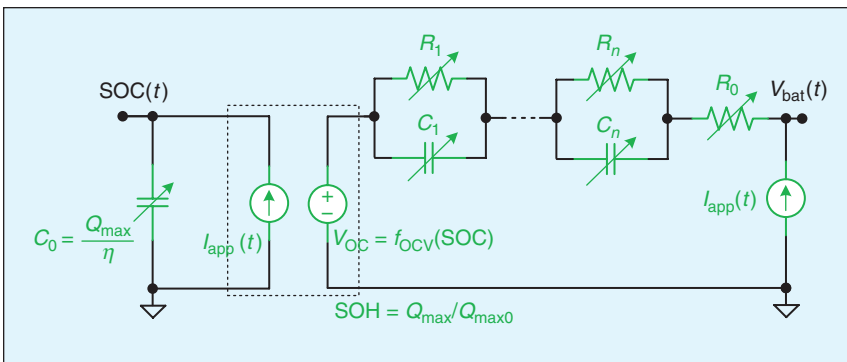


FIGURE 2 – A typical ECM of Li-ion batteries used in conventional BMSs. V_{bat} : terminal voltage; I_{app} : applied current; Q_{max} : battery capacity; Q_{max0} : battery capacity of a fresh cell; η : coulombic efficiency; V_{OC} : open circuit voltage expressed as a nonlinear function $f_{OCv}(\cdot)$ of the SOC.

$$\alpha u(z_1, t) + (1 - \alpha) \delta \frac{\partial u(z_1, t)}{\partial z} = BV_1,$$

$$\alpha u(z_2, t) + (1 - \alpha) \delta \frac{\partial u(z_2, t)}{\partial z} = BV_2,$$

and the initial condition at $t = 0$ if $M \neq 0$:

$$u(z, 0) = u_0,$$

where $u(z, t)$ represents a state variable of interest in the space $z \in [z_1, z_2]$ and at time $t \in [0, \infty)$, M is a coefficient that represents the ability to store a certain form of energy, δ is a coefficient signifying the rate of transport, ξ is the source term, u_0 is the initial value, BV_1 and BV_2 are two boundary values, $\alpha \in \{0, 1\}$ is a coefficient to determine the types of boundary conditions, and m indicates the types of coordinates associated with the PDE.

As shown in Figure 1, when $m = 0$, (1) describes the transport and conduction phenomena along the horizontal direction of a cell on the macroscale ($z = x$), while the dynamics along the remaining two dimensions perpendicular to x are ignored. For $m = 2$, (1) describes the transport of the lithium species along the pseudospherical dimension ($z = r$) on the microscale. Note that the case of $m = 1$ describes the dynamics in a cylindrical coordinate, and it is not used in the original P2D model.

Table 1 summarizes the symbols defined for different governing equations in the P2D model, where the superscripts “+”, “-”, and “sep” represent the positive electrode, negative electrode, and separator domains, respectively. For the ease of notation, we use $\pm \in \{+, -\}$ and $j \in \{+, -, \text{sep}\}$ to indicate quantities in different domains. The symbols in Table 1 and the

generalized PDE (1) define the specific governing equations (2)–(5) for the P2D model. Specifically, j_n^\pm is the pore wall molar flux between the solid phase and electrolyte, L^j is the width of a domain, ε_e^j is the volume fraction of the electrolyte, t_a^0 is the transference number, F is the Faraday constant, A is the cross-sectional area of the electrode, and c_{s0}^\pm and c_{e0} are the initial concentrations of the solid phase and electrolyte, respectively. Parameters such as the solid phase and electrolyte diffusivities ($D_{s,\text{eff}}^\pm$ and $D_{e,\text{eff}}^j$) as well as the solid phase and electrolyte conductivities (σ_{eff}^\pm and κ_{eff}^j) are usually concentration- and temperature-dependent. In addition, as indicated in Figure 1, R_p^\pm represents the radius of the assumed spherical particle in the solid phase, and $a_s^\pm = 3\varepsilon_s^\pm/R_p^\pm$ denotes the specific electrode area, where ε_s^\pm is the volume fraction of the solid phase. In (5), instead of using electrolyte potential Φ_e^j to describe the charge transport as in the original P2D model, a new potential term Φ_e^j is defined based on (6) so that the corresponding PDE can be written in the generalized form (1) [19]:

$$\Phi_e^j(x, t) := \Phi_e^j(x, t) - \left(\frac{2R_g T t_a^0}{F} \right) \ln \left(\frac{c_e^j(x, t)}{c_{e0}} \right), \quad (6)$$

where R_g and T are the universal gas constant and the cell temperature, respectively. The term U_e^j is an overpotential due to the deviation of the electrolyte concentration from its initial value c_{e0} , and we denote this nonlinear relationship as $U_e^j = f_E(c_e^j)$.

Next, the Butler–Volmer equation is used to describe the intercalation reaction kinetics during charging and discharging. It establishes a nonlinear coupling relationship between the ionic molar flux j_n^\pm and the charge transfer overpotential η_{ct}^\pm in the corresponding electrode:

$$j_n^\pm(x, t) = i_0^\pm(x, t) \left[\frac{2}{F} \sinh \left(\frac{F \eta_{\text{ct}}^\pm(x, t)}{2R_g T} \right) \right], \quad (7)$$

$$\eta_{\text{ct}}^\pm(x, t) = \Phi_s^\pm(x, t) - \Phi_e^\pm(x, t) - U_{\text{ss}}^\pm(x, t) - F r_f^\pm(x, t) j_n^\pm(x, t), \quad (8)$$

where the reaction current density i_0^\pm is expressed as a nonlinear function of c_{ss}^\pm ; c_e^\pm, r_f^\pm represents the area-specific film resistance of the SEI layer; and U_{ss}^\pm is the open circuit potential of the electrode. The notation of the Li-ion concentration at the surface of the solid particle $c_{\text{ss}}^\pm(x, t) := c_s^\pm(x, r = R_p^\pm, t)$, U_{ss}^\pm can be expressed as a nonlinear function of c_{ss}^\pm ; i.e., $U_{\text{ss}}^\pm = f_{\text{OCp}}^\pm(c_{\text{ss}}^\pm)$. This function is determined by the thermodynamic characteristics of the active materials used in the electrode. Finally, the battery terminal voltage and SOC are obtained by

$$V_{\text{bat}}(t) = \Phi_s^+(0^+, t) - \Phi_s^-(0^-, t) + R_{\text{col}} I_{\text{app}}(t), \quad (9)$$

$$\text{SOC}(t) = \frac{1}{L^-} \times \int_{0^-}^{L^-} \left[\frac{3}{(R_p^-)^3} \int_0^{R_p^-} r^2 \frac{c_s^-(x, r, t)}{c_{s,\text{max}}^-} dr \right] dx, \quad (10)$$

where R_{col} is the lumped resistance of the current collectors and $c_{s,\text{max}}^-$ is the theoretic maximum concentration in the negative electrode. Please refer to

TABLE 1 – A SUMMARY OF SYMBOLS IN THE P2D MODEL BASED ON THE GENERALIZED PDE (1).

DESCRIPTION	$u(z, t)$	z	m	M	δ	ξ	α	z_1	z_2	BV_1	BV_2	u_0	EQUATION
Mass transport (solid phase)	$c_s^+(x, r, t)$	r	2	1	$D_{s,\text{eff}}^+$	0	0	0	R_p^+	0	$-j_n^+$	c_{s0}^+	(2a)
	$c_s^-(x, r, t)$	r	2	1	$D_{s,\text{eff}}^-$	0	0	0	R_p^-	0	$-j_n^-$	c_{s0}^-	(2b)
Mass transport (electrolyte)	$c_e^+(x, t)$	x	0	ε_e^+	$D_{e,\text{eff}}^+$	$t_a^0 a_s^+ j_n^+$	0	0^+	L^+	0	$D_{e,\text{eff}}^{\text{sep}} \frac{\partial c_e^{\text{sep}}(0^{\text{sep}}, t)}{\partial x}$	c_{e0}	(3a)
	$c_e^-(x, t)$	x	0	ε_e^-	$D_{e,\text{eff}}^-$	$t_a^0 a_s^- j_n^-$	0	0^-	L^-	0	$D_{e,\text{eff}}^{\text{sep}} \frac{\partial c_e^{\text{sep}}(L^{\text{sep}}, t)}{\partial x}$	c_{e0}	(3b)
Charge transport (solid phase)	$c_e^{\text{sep}}(x, t)$	x	0	$\varepsilon_e^{\text{sep}}$	$D_{e,\text{eff}}^{\text{sep}}$	0	1	0^{sep}	L^{sep}	$c_e^+(L^+, t)$	$c_e^-(L^-, t)$	c_{e0}	(3c)
	$\Phi_s^+(x, t)$	x	0	0	σ_{eff}^+	$F a_s^+ j_n^+$	0	0^+	L^+	$-I_{\text{app}}/A$	0	–	(4a)
Charge transport (electrolyte)	$\Phi_s^-(x, t)$	x	0	0	σ_{eff}^-	$F a_s^- j_n^-$	0	0^-	L^-	I_{app}/A	0	–	(4b)
	$\Phi_e^+(x, t)$	x	0	0	κ_{eff}^+	$-F a_s^+ j_n^+$	0	0^+	L^+	0	$-I_{\text{app}}/A$	–	(5a)
	$\Phi_e^-(x, t)$	x	0	0	κ_{eff}^-	$-F a_s^- j_n^-$	0	0^-	L^-	0	I_{app}/A	–	(5b)
	$\Phi_e^{\text{sep}}(x, t)$	x	0	0	$\kappa_{\text{eff}}^{\text{sep}}$	0	0	0^{sep}	L^{sep}	$-I_{\text{app}}/A$	$-I_{\text{app}}/A$	–	(5c)

[14], [19], and [20] for more detailed descriptions of the P2D model.

The P2D model described by (1)–(10) is very general, and modifications can be made to accommodate Li-ion batteries with different chemistries, such as lithium cobalt oxide [21], lithium iron phosphate [22], lithium manganese oxide [17], lithium nickel cobalt aluminum oxide [23], and lithium nickel manganese cobalt oxide [2], [24]. Besides the intercalation/de-intercalation process described in (1)–(10), different side reaction models can be incorporated into the P2D framework to predict aging phenomena, such as increasing resistance due to SEI film growth and strain-induced cracking of solid particles, decreasing electrolyte volume fractions, and fading capacity due to SEI film growth and lithium plating, and relevant parameters can be used to define the SOH of a cell [25]. For example, the driving force of lithium plating, the side reaction potential, can be modeled by an equation similar to (8) [2], whereas it is inherently difficult for conventional ECMs to distinguish and capture localized aging characteristics. Therefore, the P2D model and its extension to incorporate aging dynamics are favorable to the development of

advanced BMSs, potentially leading to extended battery life.

Model Order Reduction Techniques

Model order reduction (MOR) approaches can be adopted to obtain simplified first-principle Li-ion battery models. The rapid pace of advancement in microprocessor technology has enabled the implementation of high-fidelity ROMs of Li-ion batteries that have a system order greater than 100 [24], and the representations have the potential to be incorporated into real-time embedded systems as “digital twins” [26]. However, model orders not much higher than that of prevailing ECMs with two to five states [27] are the most desirable in the design of many BMS functionalities, such as online state estimation [28], available power prediction [29], parameter estimation [30], cell balancing [31], and fault diagnosis [32]. The development of optimal battery control, such as fast charging for EVs, energy management for hybrid EVs (HEVs), and power flow control for grid-connected battery energy storage systems, also requires a low-order system to balance the trilemma of high charging/discharging

rates, long battery life, and ensured safety since the complexity of most of those algorithms increases dramatically as the model order increases [33]. An advanced BMS with physics-based ROMs is depicted in Figure 3.

Extensive efforts have been made to develop MOR techniques in applied mathematics. However, for the control-oriented MOR of Li-ion batteries, intuition-based techniques reported in the literature are also very effective since they avoid complex numerical recalculations of ROM parameters that are necessitated by battery degradation and nonlinearity. These ROMs can be implemented in real-time control algorithms [10]. The main control-oriented MOR techniques applied to the P2D model will be discussed in four categories in the following. A large number of the methods can be visualized and explained by reformulating the ROMs into physically meaningful equivalent circuits [19], [34], [35] so that better understanding and more insight can be provided for readers with a background in electrical and electronic engineering.

Spatial Discretization

The most straightforward and mathematically mature method to simplify a PDAE system is to employ discretization in the spatial coordinate ($z = x$ or r) to obtain a continuous-time DAE system. The DAEs are discretized in the time domain for online implementation. This strategy is usually referred to as the *method of lines*. Finite-difference methods (FDMs) [36] and finite-volume methods (FVMs) [37] are the most direct approaches in this category to simplify the equations (3)–(5) that govern macroscale variables. For the solid-phase diffusion equation (2) established in the pseudospherical coordinate, the method of lines can also be used via FDMs [38], FVMs [39], the control volume method [40], and so on. In FVMs and the control volume method, the law of mass conservation has been specifically guaranteed so that no drift effect occurs during long operations.

By applying spatial discretization to (1), a general coupled circuit network that exhibits the distributed

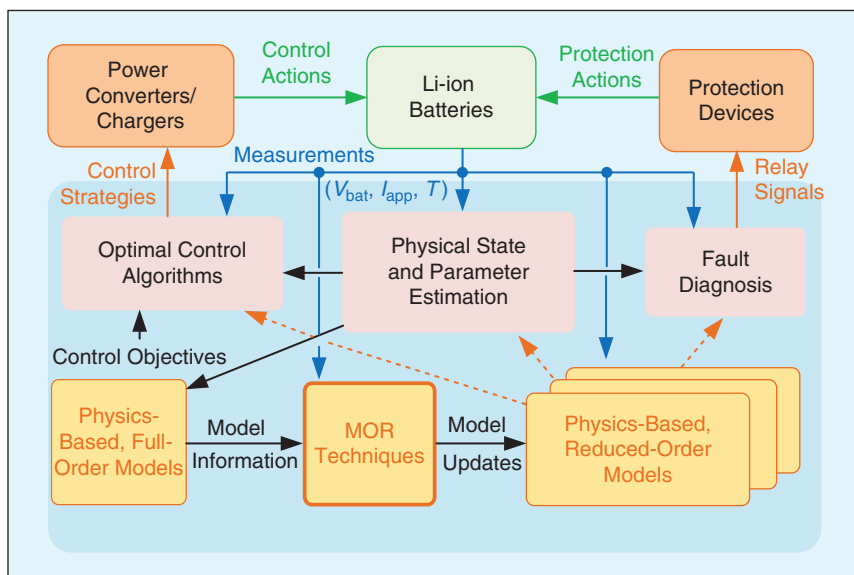


FIGURE 3 – The structure of an advanced BMS. Physics-based ROMs are used for basic BMS functions, including state/parameter estimation, fault diagnosis, and determining optimal control algorithms. State/parameter estimation guarantees that a physics-based model is sufficiently accurate during its operational lifetime. Optimal control algorithm blocks use model information and control objectives to calculate an optimal current profile for a battery. Fault diagnosis algorithms utilize estimated faulty state/parameters information to direct protection systems.

parameter nature of the P2D model can be obtained using an electrical analogy, as in Figure 4, where a subscript i is attached to indicate the variable at the i th mesh node or control volume, while the superscript to indicate the domain is dropped. This transmission-line-like general circuit representation consists of a subcircuit for the charge transport process, as shown in Figure 4(a), a subcircuit for the mass transport process in the electrolyte, as detailed in Figure 4(b), and a set of subcircuits for the mass transport in the solid phase of the electrodes, as described in Figure 4(c). These subcircuits interact with one another via the coupling components depicted in Figure 4(d). Note that battery degradation is closely related to the voltage $\Phi_{s,i} - \Phi_{e,i}$ and resistance $R_{\Sigma,i}$ on the vertical branches in Figure 4(a). Here, $R_{\Sigma,i}$ consists of the local SEI resistance $R_{SEI,i}$ [which is proportional to r_f in (8)] and the intercalation-related charge transfer resistance defined as $R_{ct,i} := \eta_{ct,i}/I_{n,i}$, where $I_{n,i} = Fa_{s,i}j_{n,i}\Delta x_i$ is the branch

current and Δx_i represents the discrete space interval in the x direction. During battery operation, various side reactions occur, which causes performance to deteriorate due to the increasing resistance $R_{SEI,i}$ and loss of cyclable lithium. Side reaction rates are mainly affected by the magnitude of the value of $\Phi_{s,i} - \Phi_{e,i}$. Therefore, accurate modeling of degradation behaviors, such as those associated with $R_{SEI,i}$ and $\Phi_{s,i} - \Phi_{e,i}$, is beneficial for battery health monitoring, diagnosis, and optimal control.

Spatial discretization methods can preserve most model properties within a wide range of operating conditions, and model extensions can be readily achieved to consider the nonuniformity of the double-layer capacitance [34], mechanical stress [41], heat accumulation and transfer [21], aging behaviors [2], [34], and so forth on different time scales. The ability to retain slow dynamics during the relaxation process is another distinguishing feature of these approaches;

i.e., after the current I_{app} is removed, the capacitor voltages in Figure 4(b) and (c) will be gradually equilibrated through a chain of interactions among subcircuits. Clearly, the complexity and accuracy of these ROMs are determined by the number and positions of the mesh points/control volumes of interest. Uneven nodes can be used to increase model fidelity [40]. Using FVMs, the simulation results in Figure 5(a) show that only a small number of discretized points is required under operating conditions with low current rates. However, as the current increases, from Figure 5(b), it can be seen that more nodes are needed to reproduce the inflated (or compounded) distributed effects and characteristics due to the saturation of concentrations. This would be difficult for model-based control system design and online implementation. MORs for large-scale interconnected circuit networks have potential to further reduce the order of discretized battery models [42].

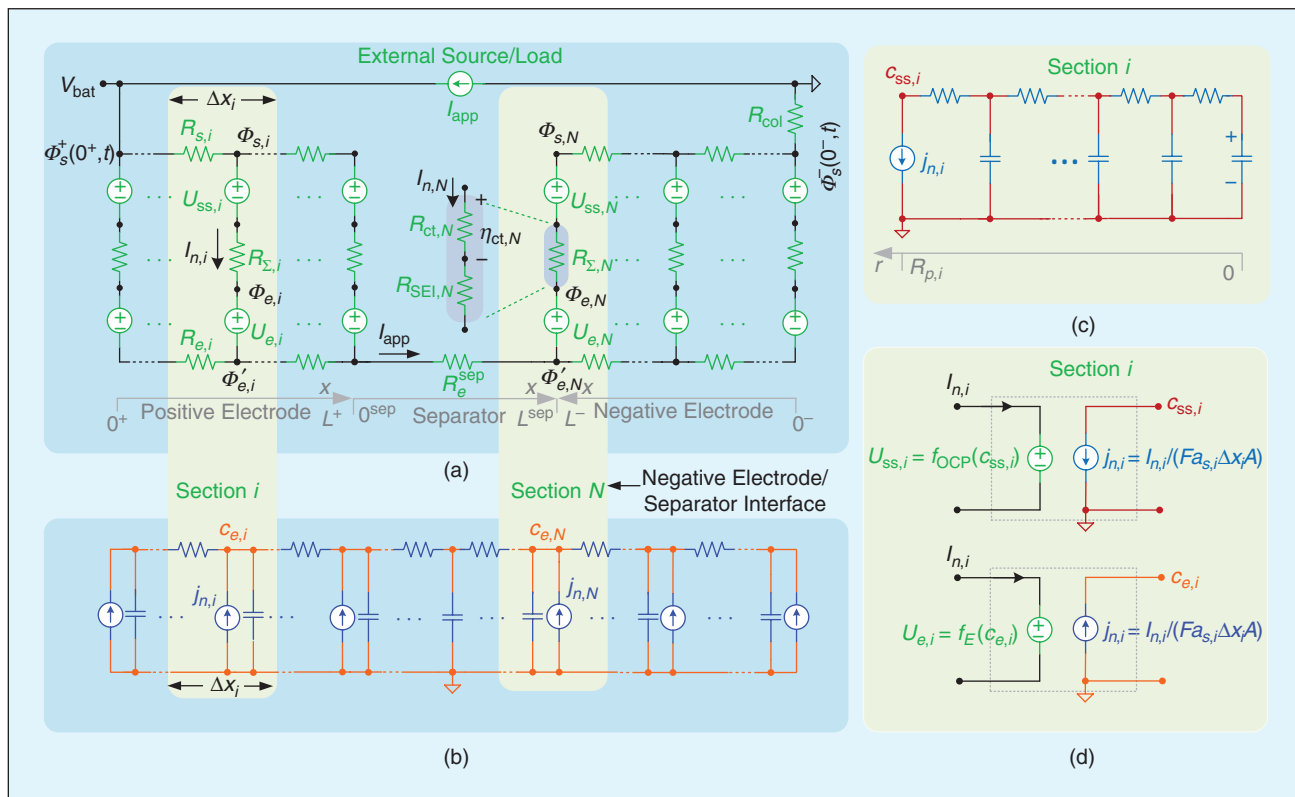


FIGURE 4 – A general distributed-parameter equivalent circuit for a P2D model obtained by spatial discretization. (a) The subcircuit for charge transport and intercalation/de-intercalation reaction kinetics. (b) The subcircuit for mass transport in the electrolyte. (c) The subcircuit in the i th section (node) in the macroscale for mass transport in the solid phase of the electrode. (d) The macroscale coupling between the charge and mass transport subcircuits on the i th section (node).

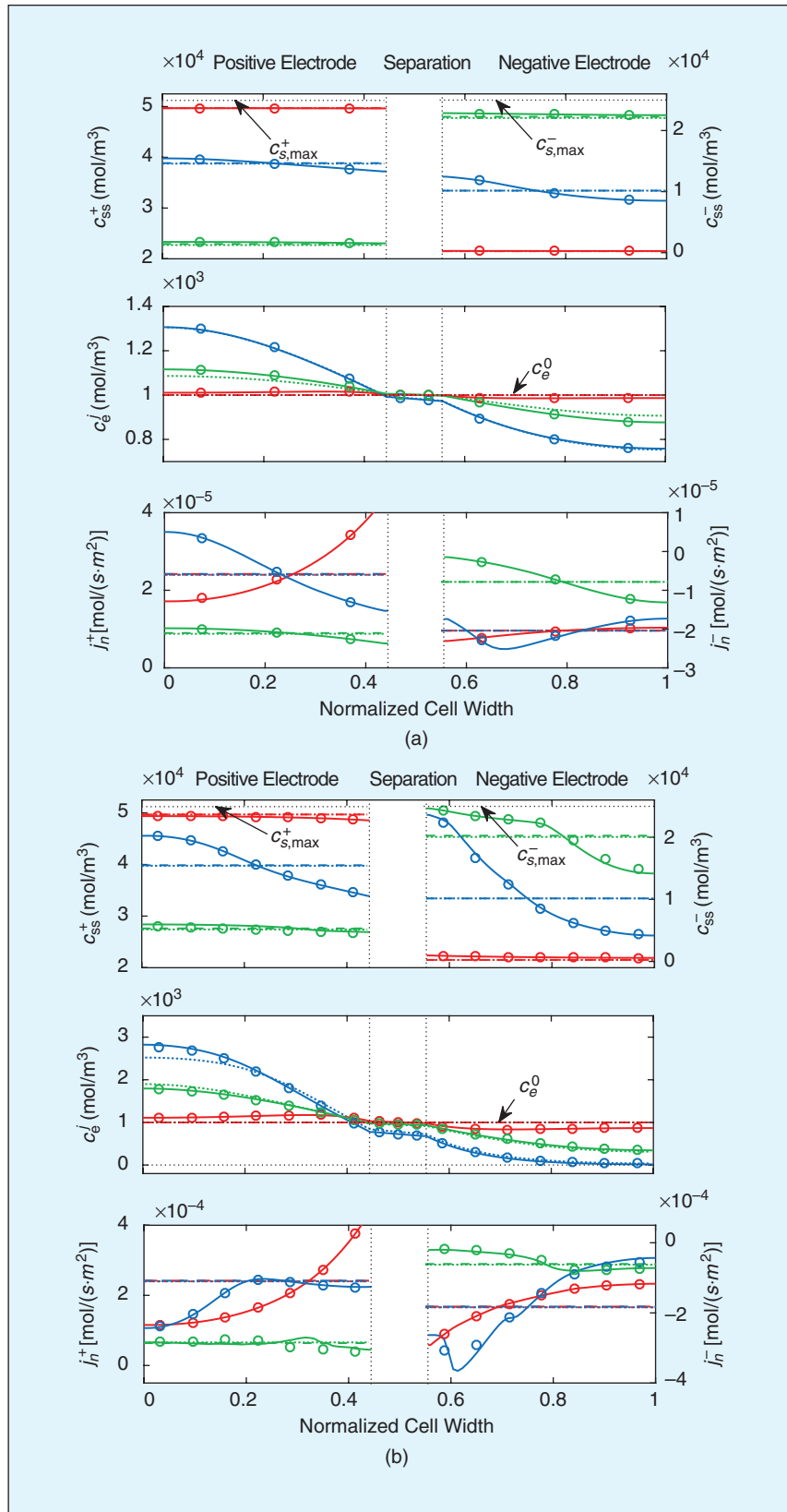


FIGURE 5 – A comparison of the spatial distributions of the solid-phase surface concentration (c_s^+), electrolyte concentration (c_e^0), and pore wall molar flux (j_n^+), simulated using different models during a constant-current (CC), constant-voltage (CV) charging process. The CC stage has (a) a low current rate and (b) a high current rate. Red indicates the early CC stage, blue represents the late CC stage, and green specifies the CV stage. Solid lines denote a P2D model, circles indicate a discretized model using an FVM, dashed lines specify an SPM, and dotted lines show an enhanced SPM.

Function Approximation

The second category of methods approximates spatiotemporal variables by a finite weighted sum of assumed functions in the form of

$$u(z, t) \approx \sum_{k=0}^N \alpha_k(t) f_k(z). \quad (11)$$

The objective is to find the time-varying coefficients $\alpha_k(t)$ for selected trial functions (or basis functions) $f_k(z)$ so that the residual $\mathcal{R}(z, t) = u(z, t) - \sum_{k=0}^N \alpha_k(t) f_k(z)$ has certain properties that enable one to minimize approximation errors. Trial functions are usually selected as *constant*, *power*, *sinusoidal*, *logarithm*, *polynomial*, or a combination the five, and they are generally chosen to ensure that boundary conditions are automatically satisfied. They are sometimes referred to as *projection-based methods*, where trial functions and weights can be obtained via optimization, e.g., by minimizing the Euclidean norm error in the frequency domain [43] and via applying eigenfunction/singular value decomposition to a data ensemble obtained from the full-order model [39].

Many of these approaches are known as *spectral methods*, where the integral of the weighted residual across the domain $[z_1, z_2]$ of z should vanish; i.e.,

$$\int_{z_1}^{z_2} w_k(z) \mathcal{R}(z, t) dz = 0$$

$$k \in \{0, 1, \dots, N\}, \quad (12)$$

where the weights $w_k(z)$ are called *test functions*. In Galerkin methods [44], the test functions equal the trial functions $f_k(z)$. Cosine functions [44], Chebyshev polynomials [45], and Legendre polynomials [46], [47] are usually chosen as trial and test functions in spectral methods due to their good characteristics for nonperiodic signal reconstruction. In orthogonal collocation methods and pseudospectral methods [45], [48], [49], the test functions are the Dirac delta functions defined at specific locations (namely, the collocation points). Spectral methods' accuracy can be improved by increasing approximation order N but at the expense of drastically

increased complexity in analytically deriving ROMs.

With the consideration of constraints such as the boundary conditions, conservation of mass, and geometrical properties of the solution, heuristic methods can also be used to select trial functions to simplify the determination of the coefficients. Only a small set of trial functions needs to be used, so the resulting model can be explicitly expressed as functions of battery parameters. For example, in approximating the solid-phase concentration PDE (2), the solid-phase concentration c_s^\pm can be assumed as a polynomial function of the radial position r with only even degree terms. The coefficients $\alpha_k(t)$ in (11) are obtained as functions of several physically meaningful quantities, such as the volume-averaged concentration $c_{s,avg}^\pm$ and the volume-averaged concentration flux as well as the surface concentration c_{ss}^\pm . This leads to a two- or three-parameter polynomial profile approximation [50], which can be illustrated using the equivalent circuits in Figure 6(a) and (b). This method is valid when the effective diffusion coefficient $D_{s,eff}^\pm$ of the solid phase is either a constant or a function of the solid-phase concentration [51], and it performs well under constant, long, low-to-medium current rate applications.

However, there can be significant approximation errors under high current rate and high-frequency applications, such as fast EV charging [52], HEV pulse operations [53], and the provision of fast frequency response for grid systems [54]. Higher-order approximations are needed to more accurately describe the increased spatial nonuniformity in the solid particles. The polynomial profile concept has also been applied to the macroscale approximation of the electrolyte concentration and potential [55], molar flux, solid-phase concentration, and conductivity of electrolytes [21]. However, on the macroscale, the polynomial profile assumption can fail during dynamic operation at high rates and at the end of the charge/discharge process. For example, in fast charging, the local solid-phase

concentration near the separator and the local electrolyte concentration tend to saturate close to their physical and safety limits, and low-order approximation is unlikely to precisely describe the situation. High-order approximation is necessary, although the derivation of the coefficients can be much more complicated.

Frequency Domain Approximation

Transfer functions are essentially control-oriented and can be readily realized in state–space forms for linear control system design. For the MORs techniques in this category, the main objective is to find a rational transfer function between the input current I_{app} and the local variable of interest, such as concentrations and overpotentials. Since (1) represents an infinite-order system, the transfer function between any state u and the input (the source ξ or a boundary value; see Table 1) is transcendental. For example, the analytical result for the solid-phase diffusion equation (2) can be obtained by applying a Laplace transform to (1), with the consideration of its boundary conditions; i.e., [27]

$$\frac{c_{ss}^\pm(x,s)}{j_n^\pm(x,s)} = \frac{R_p^\pm}{D_{s,eff}^\pm} \times \frac{\tanh(R_p^\pm \sqrt{s/D_{s,eff}^\pm})}{\tanh(R_p^\pm \sqrt{s/D_{s,eff}^\pm}) - R_p^\pm \sqrt{s/D_{s,eff}^\pm}}. \quad (13)$$

However, as the equations in the P2D model are highly nonlinear and tightly coupled, additional steps are needed to identify the relationship between the current I_{app} and the local molar flux j_n [which is proportional to the branch current $I_{n,i}$ in Figure 4(a)]. Assumptions are usually made to decouple the submodels, e.g., by assuming a spatially uniform molar flux distribution ($j_n^\pm(x,t) = \pm I_{app}(t)/(Fa_s^\pm L^\pm A)$) in the electrode and considering constant electrolyte concentrations ($c_e^j(x,t) = c_{e0}$) [27].

MOR methods are applied to transcendental transfer functions to find rational transfer functions as required. Among various MOR approaches, the eigenfunction technique analytically calculates all the periodic roots of the

transcendental transfer function, and the resulting infinite series is truncated to obtain a ROM [56]. Similarly, in the residue grouping method, all periodic poles and zeros will be calculated and truncated; the poles will be first grouped and approximated with new ones by minimizing a frequency response cost function via nonlinear optimization techniques [27]. Compared to the eigenfunction method, residue grouping can offer improved frequency response accuracy in a wide range. However, it is less implementable for real-time systems, as it is computationally inefficient and sensitive to initial guesses and there are no guaranteed convergence and global optimality.

In contrast, in the Padé approximation, transcendental transfer functions are linearized into rational ones in the s domain so that the system order can be directly reduced by moment matching [57]. The coefficients of these rational polynomials consist of physical cell parameters and can be readily updated according to any change in operational conditions. Accuracy is further improved by increasing the order of the rational transfer functions that are used. There is a tradeoff between the required level of accuracy and the computational overhead, as the model order increase eventually imposes additional requirements. Low-order Padé approximations provide sufficiently accurate results for stationary battery applications, and higher-order ones can be used for EVs [58].

A transfer function can be expressed in different impedance forms, depending on the realization strategies to obtain a state–space model. For the solid-phase diffusion equation (2), a general equivalent circuit based on diagonal canonical realization is presented in Figure 6(c), where the surface concentration $c_{ss,i}$ is expressed as the sum of the volume-averaged concentration $c_{s,avg,i}$ and a series of concentration deviation terms. With the uniform molar flux assumption, a circuit for the electrolyte diffusion equation (3) can be derived, and it is shown in Figure 6(d). Similar to the

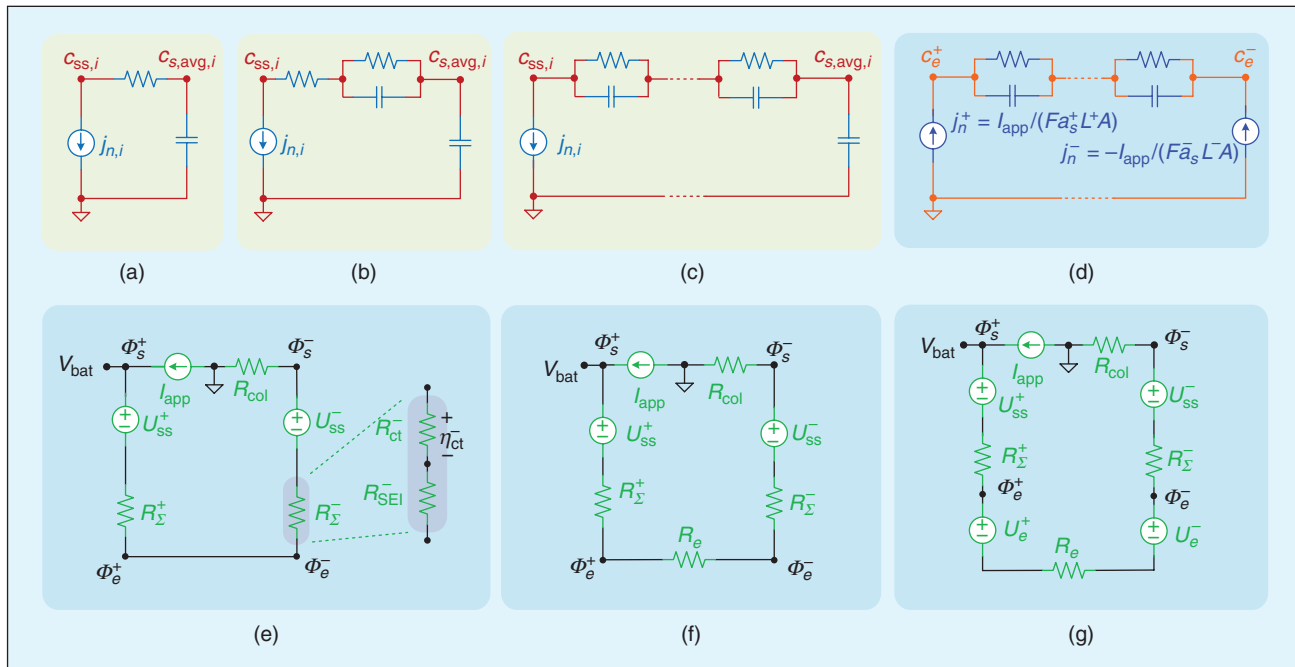


FIGURE 6 – Circuits equivalent to (a) two-parameter polynomial approximation, (b) three-parameter approximation, and (c) a diagonal canonical form realization of Padé approximation, residue grouping, and so on, obtained using the diagonal canonical realization. (d) Electrolyte concentration dynamics based on Padé approximation and uniform molar flux. The (e) single particle model (SPM), (f) electrode averaged model, and (g) SPM with an electrolyte.

method of lines presented in the “Spatial Discretization” section, continuous-time ROMs obtained from residue grouping and Padé approximation need to be discretized in the time domain for control system implementation. In contrast, the dynamic realization algorithm directly generates an optimal reduced-order, discrete-time state–space realization from the original PDE by first finding the discrete-time pulse response and then using the Ho–Kalman algorithm to compute the state–space realization [59]. Several improved linear discrete-time models based on such a realization process are investigated and compared in [60], whose authors conclude that they all are more computationally efficient than the dynamic realization algorithm while requiring less memory, although it is difficult to directly relate the model parameters to any physical meaning [45].

The derivation of ROMs from frequency domain analysis is usually labor-intensive, although the resulting models are easy to implement. Since it is necessary only to evaluate the variables at specific locations of interest within a battery, the computational

burden can be lower than the spatial discretization methods, where all locations need to be considered at the same time. However, as there is no guarantee that the transfer functions for different variables share the same poles, the order of the ROMs can be high to achieve model precision if a large number of internal variables needs to be simultaneously investigated. Furthermore, as assumptions are made and linearization steps are taken in such small-signal methods, the fidelity of the ROMs can be low in extreme operating conditions with persistent applied current rates, such as fast charging. Relaxing the small perturbation assumptions can lead to much more complex modeling processes [61].

Simplified Physics/Spatial Lumping

In many physics-based Li-ion battery ROMs, assumptions are made by fully or partially ignoring macroscale dynamics effects under specific operating conditions. In electrodes, this leads to uniform molar flux, and such assumptions have been extensively adopted in combination with the techniques in the previous categories,

e.g., those described in the “Function Approximation” and “Frequency Domain Approximation” sections. This way, complex physical dynamics and strong coupling relationships between different submodels can be significantly simplified.

The single particle model (SPM) assumes uniformity for all local variables in each electrode and a negligible impact from the variation of the electrolyte concentration and potential on the terminal voltage [51]. This tends to be valid under relatively low current rates and for cells with thin electrodes. To illustrate, consider that in Figure 4(a), when the electrode is very thin, the injected current rate and thus the branch currents flowing through the solid-phase resistance $R_{s,i}$ and electrolyte resistance $R_{e,i}$ are low. This results in negligible differences in local potentials and currents. In addition, under the assumption $c_{e,i} = c_{e0}$, the voltage sources $U_{e,i}$ can be deleted from the circuit since, according to (6), $U_{e,i}$ is proportional to $\ln(c_{e,i}/c_{e0})$. This renders a simplified lumped-parameter ECM for the SPM, as in Figure 6(e). In the literature, it is shown that the maximum applicable

current rate is usually 1 C for a high-power battery with thin electrodes and 0.5 C for a typical high-energy battery that has a wider electrode [14]. (The 1-C current rate is defined as the current through a battery divided by the theoretical current draw under which the battery would deliver its nominal rated capacity in 1 h. It has the units of h^{-1} .) Hence, the SPM is generally not recommended for high-power applications, such as fast EV charging and HEV operation involving high power pulses [14], but it is well-suited to many grid applications [62], [63] and daily EV driving, where the operating ranges are much narrower.

Similar to the SPM, an electrode averaged model was developed in [38] by averaging distributed variables in electrodes. It couples the average solid material concentration with the average values of the chemical potentials, electrolyte concentration, and current density, as demonstrated in Figure 6(f). Electrolyte dynamics are considered sufficiently fast compared to the diffusion process in electrodes, and therefore they can be modeled as purely resistive in nature, as in Figure 6(f). The electrolyte concentration is considered constant for electrochemical state observer design [64]. Further improvement of the SPM and the electrode averaged model was made by adding the effect of the distributed electrolyte concentration and potential variations. For example, the enhanced, or extended, SPM (ESPM) [55], [65] and the SPM with electrolytes [66] were developed based on the concepts of spatially lumping certain quantities. They can be illustrated using the ECM in Figure 6(g), where the impact of the electrolyte concentration variation and electrolyte potential is embodied by lumped voltage source U_e^\pm and electrolyte resistance R_e .

Comparison of MOR Techniques

In the literature, the MOR methods presented in the previous section have been applied to achieve various BMS functionalities, including state/parameter estimation, fault diagnosis, and optimal control. Relationships between MOR approaches are

documented in Figure 7, and the methods' strengths, weaknesses, and possible applications are summarized in Table 2. From the table, it is clear that spatial discretization methods are the most direct and widely applicable for obtaining accurate results, and model accuracy can be improved by increasing the number of discretization nodes and control volumes. For some function approximations, it is possible to increase ROM fidelity by assuming a more complex basis function with a higher order. A spectral method can achieve the same accuracy as a discretization approach, with much fewer discretization nodes, typically with a reduction factor of ten to 100, provided the solution is sufficiently smooth in the space domain [45].

As for frequency domain techniques, the derivation procedures are considerably more complex, especially for obtaining transcendental transfer functions. Matching a wide frequency range also requires high-order approximations. Since frequency domain methods rely heavily on the assumption that a system is linear, their accuracy cannot be enhanced much in situations when large signals are involved. However, the techniques can be suitable for applications in

which a battery cycles around a specific level in the mid-SOC region, such as HEVs and grid frequency control. If the uniform assumption about spatially distributed variables proves to be invalid, it is impossible to improve ROM accuracy by increasing the model orders.

The SPM is one of the most simplified electrochemical model frameworks, requiring very low computation and providing sufficient model accuracy for applications limited to low and medium current rates. It can be considered a special spatial discretization model, with only one control volume or node for each electrode. ESPMs enhance the SPM by incorporating concentration and potential variations inside a cell. As a result, the ESPM span of applicability is increased by providing sufficiently accurate results under high current rates and with a substantially lower computational burden than the P2D model.

In a practical ROM, the MOR techniques are usually blended. This is because a combination can potentially offer improved balance between model accuracy and computational complexity. In addition, prior knowledge of physical constraints and assumptions, such as the shape of the

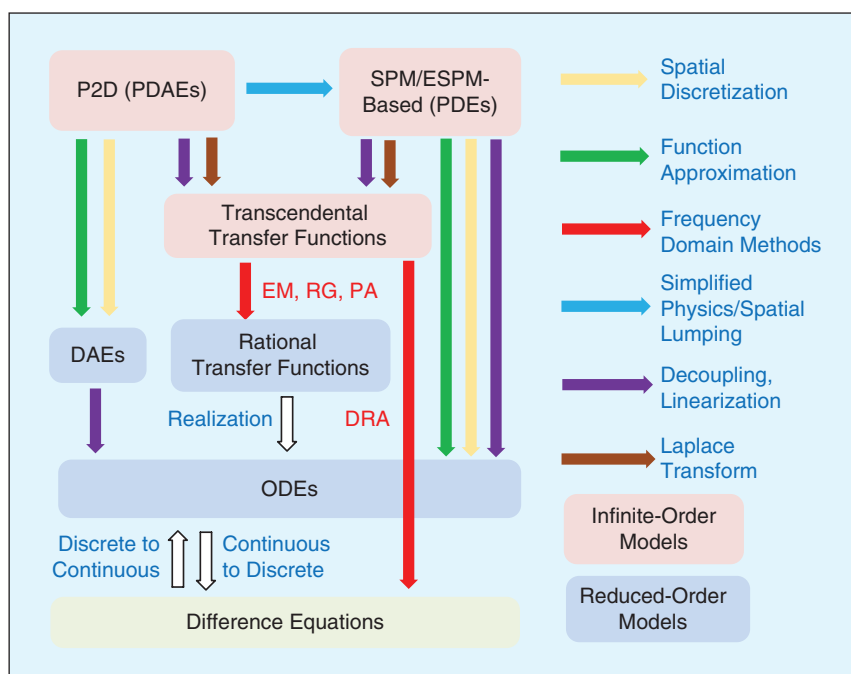


FIGURE 7 – Relationships between major MOR techniques for the P2D model. EM: eigenfunction method; RG: residue grouping; PA: Padé approximation; DRA: dynamic realization algorithm.

TABLE 2 – STRENGTHS, WEAKNESSES, AND APPLICATIONS OF TYPICAL MOR TECHNIQUES FOR PHYSICS-BASED L-ION BATTERY MANAGEMENT.

MOR CATEGORY	TYPICAL MOR TECHNIQUE	STRENGTHS	WEAKNESSES	APPLICATIONS OF ROMS IN ADVANCED BMSs				
				SOC/ELECTROCHEMICAL STATE ESTIMATION	SOH/PARAMETER ESTIMATION	REAL-TIME CHARGING CONTROL	CHARGING PROFILE OPTIMIZATION	OTHERS
Spatial discretization	FDM	Easy to implement, generic to all operating conditions	High computation, not mass conservative	[38], [70]–[72]	[73]	[52], [74], [75]	–	–
	FVM, control volume method	Easy to implement, generic for all operating conditions, mass conservative	High computation	[37], [76]	[77]	[78]	[79]	–
Function approximation	Spectral (e.g., Galerkin method, orthogonal collocation)	Low computation for smooth profiles	Complex derivation and implementation	[45]	[80], [81]	[49], [82]	[83]	–
	Polynomial profile approximation	Easy to implement	Subject to low-to-medium rates	[37], [84]–[89]	[81], [86], [88]	[33], [75], [78]	[90]	[7] (renewable energy dispatch)
Frequency domain approximation	Eigenfunction methods	Easy to implement	Linear (small-signal) model	[37], [88]	[88]	–	–	–
	Residual grouping	High accuracy across wide operating ranges	Need to solve nonlinear optimization problems, linear model	[53]	[91]	[92]	[90], [93]	–
Simplified physics/spatial lumping	Padé approximation	Easy to implement, high accuracy	Linear model	[72], [94]	[94], [95]	[74]	[96], [97]	[98] (HEV energy management)
	Direct realization algorithms	Low computation, easy to implement	Labor-intensive linear model derivation	[99]	–	[100]	–	–
	SPM-based	Low computation, easy to implement	Narrow operating range, not suitable for high-rate applications	[38], [70], [84], [86], [89], [94], [101]–[103]	[73], [86], [94], [101], [103]	[82]	[97], [104]	[32] (fault diagnosis)
	ESPM-based (improved with electrolyte model)	Low computation, enhanced accuracy at higher rates	Not suitable for cells with wide electrode	[28], [72], [85]	[28], [30]	[33]	[90], [96], [105]	[98] (HEV energy management)

solution, the conservation of the mass and charge, the satisfaction of boundary conditions, volume-average values, continuity, and so on, is useful for developing a proper ROM for a specific application. Special consideration for P2D ROMs should be paid to the Butler–Volmer equation (7), as it imposes an algebraic constraint. This adds computation difficulty in solving models if the ROMs are DAEs since, in each time step, an iterative method has to be used to obtain a reasonably accurate solution. Linearization is often employed to remove such an algebraic constraint, with an approximated charge transfer resistance R_{ct} , and this is essentially carried out in frequency domain methods.

As an example, Figure 8 compares the frequency response and time domain pulse current response for the solid-phase diffusion equation (2b) by using several typical MOR techniques, and in the legend, numbers in parentheses indicate the model order. In Figure 8(a), the ideal frequency response is calculated using the transcendental transfer function (13), and it shows that most ROMs can capture characteristics in the low-frequency region and with very low-order approximation, while the system order has to be increased for a wider frequency response range. In this example, Padé approximation shows superior effectiveness compared to spatial discretization and function approximation methods: the third-order Padé approximation outperforms all other tested ROMs of the same model order, and it is even more accurate than 10th-order FVMs. However, the results cannot be simply extrapolated to the full P2D model since MOR fidelity can be significantly affected by other governing equations and parameters.

In the literature, the feasible operating range of a ROM is usually indicated by the maximum applicable current rate, provided certain requirements for model accuracy (e.g., voltage errors) are met. However, since the efficacy of a MOR technique heavily depends on the underlying assumptions imposed on the battery parametric values under specific operating

conditions, when developing a ROM for BMS functions, it is less rigorous to select MOR techniques simply based on conclusions drawn from such a comparison of current rates. Instead, a general procedure to select suitable MOR techniques for deriving a ROM in BMS applications is suggested as follows:

- 1) Obtain prior knowledge of a battery's characteristics, including the cell chemistry, the rate capability, and the parameter set of the physics-based model.
- 2) Identify the operating conditions and characteristics of the current and power profiles, e.g., the maximum magnitude and bandwidth (frequency range) of the current. For applications where a Li-ion battery is likely to work closer to its endurance limits, nonuniform behaviors in the electrode become more significant, and thus a higher-dimensional ROM might be needed.
- 3) Select an infinite-order model as a benchmark; it can be a PDE- or

PDAE-based one, such as the P2D, SPM, and ESPM models, as indicated in Figure 7. Simulate the benchmark based on selected input current profiles for specific applications. Obtain the computed results of the battery variables of interest (a time series or spatial profile), and use them to validate the ROM accuracy. Make assumptions based on simulation results.

- 4) Select MOR methods and apply the algorithms to a submodel of the P2D model. Perform simulation using the reduced-order submodels, and compare the results with those obtained using the benchmark.
- 5) Evaluate the performance of the ROM by comparing it with the full-order model.

Please refer to simulation tools for ROM algorithm development and performance evaluation, with the P2D model serving as the benchmark. The tools include commercial software, such as MATLAB/Simulink, COMSOL Multiphysics, and GT-AutoLion, as

well as open source packages, such as Dualfoil (Fortran) [67], fastDFN (MATLAB) [68], LIONSIMBA (MATLAB) [20], and PyBaMM (Python) [69].

Challenges and Outlook

Pack-Level, Physics-Based Models

Because of power and capacity limits, a large number of individual cells has to be connected in series and parallel to meet high-power and high-energy requirements in many practical applications. However, even new battery cells of the same type have inevitable variations in terms of their capacity, internal resistances, and SOC, among other parameters, due to imperfections in manufacturing processes. Inconsistencies may be amplified and propagated during subsequent battery operations. Therefore, battery pack performance cannot be determined simply by adding up each in-pack cell's results. In fact, pack performance is usually limited by the weakest cell. When implementing battery models

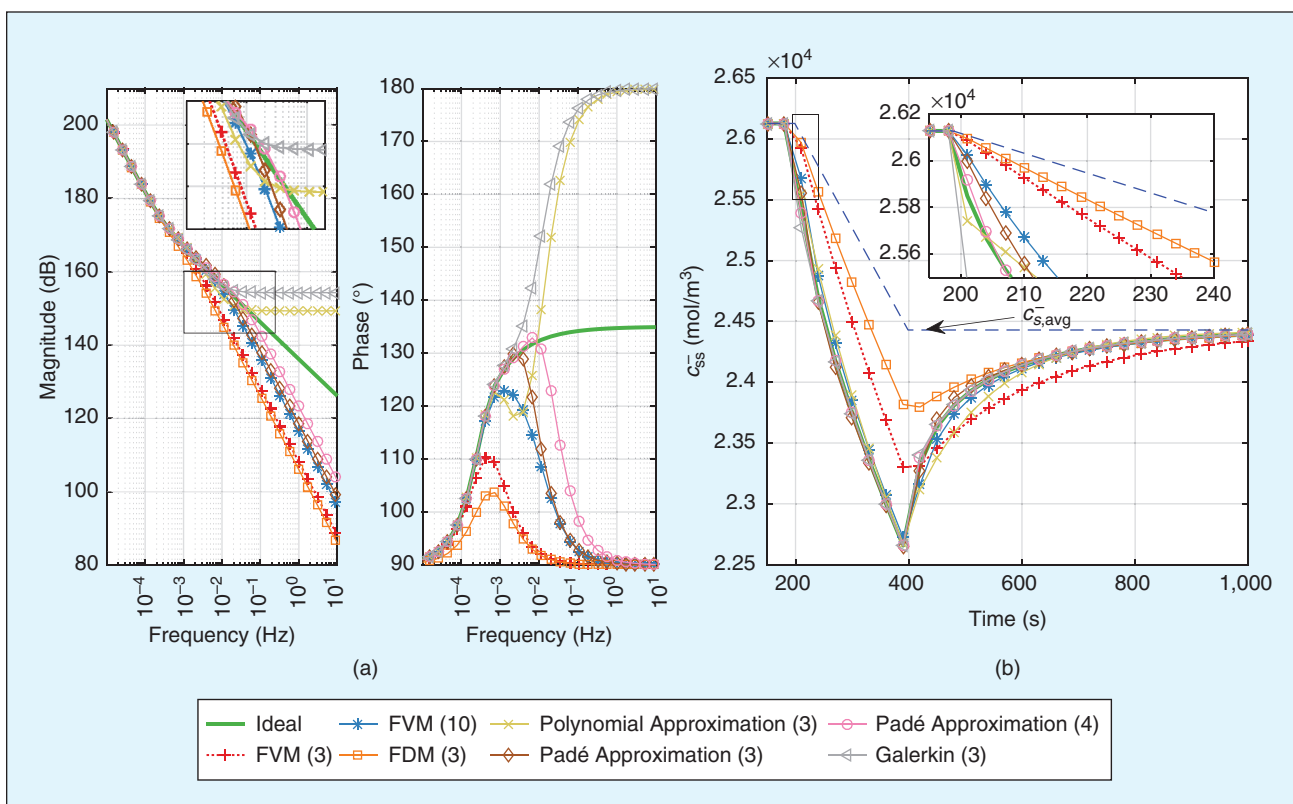


FIGURE 8 – A comparison of different MORs applied to the solid-phase diffusion (2b) of the negative electrode. (a) The frequency response. (b) The transient of the surface concentration under 1 C pulse-discharging current. In the legend, the number in parentheses indicates the model order. The parameters for the simulation are $R_p = 4 \times 10^{-6}$ m, $D_{s,eff} = 3.9 \times 10^{-15}$ m²/s, and $C_{s,max} = 30,555$ mol/m³. The magnitude of the molar flux pulse between 200 and 400 s is $j_n^- = -1.13 \times 10^{-5}$ mol/(m² · s).

in a BMS, appropriate parametric values of a physics-based model need to be selected consistent with different types of battery chemistry.

Sophisticated physics-based, pack-level battery models will require high computational power and large memory capacities to store processed data. Moreover, in practice, cell inconsistencies may create electrical imbalances [106], and thus additional circuitry [107] and control mechanisms [31], [78] are required. Therefore, there is a strong need to develop efficient physics-based, pack-level battery models to deal with cell inconsistency. Furthermore, models must be computationally efficient to cater to online applications. Pack-level, physics-based modeling poses a technical challenge to developing advanced BMSs. On the other hand, addressing the problem means all the benefits of physics-based models can be scaled up to fundamentally improve battery performance. This is considered a future research topic and requires expertise in electrochemistry, mathematical modeling, and computational science.

Long-Term Prediction of Degraded Performance

Although physics-based models are promising for predicting battery charging/discharging behavior and providing health- and safety-related information for control systems under a wide range of operational conditions, their ability to accurately predict a battery's long-term aging trajectory and remaining life needs further investigation and evaluation. Indeed, during the past two decades, degradation mechanisms have been intensively explored; however, the quantification of all the aging mechanisms and development of battery degradation models regardless of cell chemistries is an active research area. In view of recent advances in big data and artificial intelligence, data-driven modeling enabled by various machine learning techniques is considered a favorable approach [108]. In the past few years, a large number of data-driven models for SOH estimation and

remaining useful life prediction has emerged through artificial neural networks [109], Bayesian nonparametric algorithms [110], and support vector machines [111]. They work well when sufficient battery health data are available but may suffer from scalability problems due to cell-to-cell variations.

In [108], Severson et al. developed a comprehensive data set from 169 commercial Li-ion battery cells cycled under 72 different fast-charging conditions. The data were used to classify the cells at very early stages by using machine learning, in which prior knowledge of battery degradation mechanisms was ignored. The authors reported error rates of less than 10%. Since physics-based models can provide more interpretable information for feature extraction, the hybridization of physics-based and data-driven modeling techniques [112], potentially with the incorporation of implantable sensing technologies [113] for enhanced internal state observability, will bring fruitful outcomes for the development of health-aware battery management strategies.

Parameterization

Parameter identification for physics-based battery models lays a foundation for accurate state estimation and optimal control design. Due to the complexity of high-order physical models and the presence of large sets of parameters, the task of parameter identification is challenging. It has been theoretically shown that the P2D model and many of its ROMs are overparameterized [114], [115], so it is impossible to simultaneously identify all the model parameters. Furthermore, many parameters are weakly identifiable from current and voltage measurements. In light of these aspects, it is necessary to conduct sensitivity analysis, parameter grouping, and optimal experimental designs. Parameter grouping requires a detailed analysis of a model's structure and a theoretical study of identifiability [114]. Clearly, the parameterization problem becomes even more challenging when a large number of cells with different characteristics is

considered in a pack configuration and when only pack-level measurements are available.

Interestingly, for the physics-based equivalent circuits in Figures 4 and 6, since circuit parameters, such as resistances and capacitances, are always expressed as functions of electrochemical parameters, intrinsic grouping schemes have been established to simplify parameter estimation [35]. In addition, model parameters can be significantly affected by factors such as cell temperature and pack geometry. Nonuniform temperature distribution in a large battery pack can lead to a heterogeneity problem, which can cause inconsistent battery parameters across the cells and the pack. Overall, the parameterization of a coupled electrochemical and thermal model for lifelong battery management is still an active area of research.

Conclusion

Physics-based models can be considered the core of sophisticated health- and safety-aware algorithms for next-generation BMSs for Li-ion batteries. To simplify model complexity, many MOR approaches for electrochemical models of Li-ion batteries have been proposed. The techniques are categorized as spatial discretization, function approximation, frequency domain approximation, and simplified physics/spatial lumping methods. Selecting the most appropriate battery MOR techniques to develop health- and safety-aware control algorithms is crucial to achieving enhanced battery performance and extended battery life.

A ROM needs to have the ability to incorporate aging effects, temperature variations, environmental impacts, and operating conditions. Due to the highly complex physical dynamics inside a Li-ion battery cell and significantly different operating conditions in various applications, combining MOR techniques is inevitable for developing a state-of-the-art, reduced-order Li-ion battery model for a specific BMS functionality. Detailed simulations of a full-order

battery model are needed before the selection of specific MOR techniques. More effort has to be made to achieve pack-level modeling that considers cell inconsistency, efficient model parameterization, and long-term aging prediction, possibly through hybridization with data-driven techniques, such as machine learning.

Acknowledgments

This work was supported, in part, by European Union-funded Marie Skłodowska-Curie Actions Individual Fellowships, under grant 895337-Bat-Con-H2020-MSCA-IF-2019, and the Swedish Research Council, under grant 2019-04873.

Biographies

Yang Li (yangli@ieee.org) earned his Ph.D. degree in power engineering from Nanyang Technological University, Singapore, in 2015. He is a researcher in the Department of Electrical Engineering, Chalmers University of Technology, Göteborg, 41296, Sweden. His research interests include the modeling and control of battery systems in grid systems and the transportation sector. He was a recipient of the European Union Marie Skłodowska-Curie Action Individual Fellowship for battery research in 2020. He is a Member of IEEE.

Dulmini Karunathilake (r.ralaha.milage@qut.edu.au) earned her B.Sc. degree in electrical and electronic engineering from the University of Peradeniya, Sri Lanka, in 2015. She is pursuing her Ph.D. degree in the School of Electrical Engineering and Robotics, Queensland University of Technology, Brisbane, 4001, Australia. Her research interests include lithium-ion battery modeling, battery management systems, and the health-conscious optimal control of lithium-ion batteries. She is a Student Member of IEEE.

D. Mahinda Vilathgamuwa (mahinda.vilathgamuwa@qut.edu.au) earned his Ph.D. degree from the University of Cambridge, United Kingdom. He is a professor of power engineering at Queensland University of Technology, Brisbane, 4001, Australia.

His research interests include battery modeling and control, wireless power transfer, and electromobility. He is a Fellow of IEEE.

Yateendra Mishra (yateendra.mishra@qut.edu.au) earned his Ph.D. degree in electrical engineering from the University of Queensland, Australia, in 2009. He is a senior lecturer and Advance Queensland Research Fellow in the School of Electrical Engineering and Robotics, Queensland University of Technology, Brisbane, 4001, Australia. His research interests include distributed energy generation, distributed energy storage, power system stability and control, and smart grid applications. He is a Senior Member of IEEE.

Troy W. Farrell (t.farrell@qut.edu.au) earned his Ph.D. degree in mathematics from Queensland University of Technology, Brisbane, 4001, Australia, in 1998, where he is a professor in the School of Mathematical Sciences. His research interests include industrial and applied mathematical modeling and simulation, electrochemical systems, and multiscale porous media.

San Shing Choi (sanshing.choi@qut.edu.au) earned his Ph.D. degree in electrical engineering from the University of Canterbury, Christchurch, New Zealand, in 1976. He is an adjunct professor at Curtin University of Technology, Perth, Australia, and Queensland University of Technology, Brisbane, 4001, Australia. His research interests include power system control, renewable energy, and energy storage systems.

Changfu Zou (changfu.zou@chalmers.se) earned his Ph.D. degree in automation and control engineering from the University of Melbourne, Australia, in 2017. He is an assistant professor in the Automatic Control Group, Chalmers University of Technology, Göteborg, 41296, Sweden. His research interests include the intelligent management of energy systems and electric vehicles. He serves as an editor of *IEEE Transactions on Vehicular Technology* and an associate editor of *IEEE Transactions on Transportation Electrification*. He is a Member of IEEE.

References

- [1] X. Hu, C. Zou, C. Zhang, and Y. Li, "Technological developments in batteries: A survey of principal roles, types, and management needs," *IEEE Power Energy Mag.*, vol. 15, no. 5, pp. 20–31, Sept./Oct. 2017. doi: 10.1109/MPE.2017.2708812.
- [2] X.-G. Yang, Y. Leng, G. Zhang, S. Ge, and C.-Y. Wang, "Modeling of lithium plating induced aging of lithium-ion batteries: Transition from linear to nonlinear aging," *J. Power Sources*, vol. 360, pp. 28–40, Aug. 2017. doi: 10.1016/j.jpowsour.2017.05.110.
- [3] H. Rahimi-Eichi, U. Ojha, F. Baronti, and M. Chow, "Battery management system: An overview of its application in the smart grid and electric vehicles," *IEEE Ind. Electron. Mag.*, vol. 7, no. 2, pp. 4–16, June 2013. doi: 10.1109/MIE.2013.2250351.
- [4] M. Bercibar, I. Gandiaga, I. Villarreal, N. Omar, J. van Mierlo, and P. van den Bossche, "Critical review of state of health estimation methods of Li-ion batteries for real applications," *Renew. Sustain. Energy Rev.*, vol. 56, pp. 572–587, Apr. 2016. doi: 10.1016/j.rser.2015.11.042.
- [5] K. Li, F. Wei, K. J. Tseng, and B. Soong, "A practical lithium-ion battery model for state of energy and voltage responses prediction incorporating temperature and ageing effects," *IEEE Trans. Ind. Electron.*, vol. 65, no. 8, pp. 6696–6708, Aug. 2018. doi: 10.1109/TIE.2017.2779411.
- [6] Z. Wei, J. Zhao, R. Xiong, G. Dong, J. Pou, and K. J. Tseng, "Online estimation of power capacity with noise effect attenuation for lithium-ion battery," *IEEE Trans. Ind. Electron.*, vol. 66, no. 7, pp. 5724–5735, July 2019. doi: 10.1109/TIE.2018.2878122.
- [7] Y. Li et al., "Design of minimum cost degradation-conscious lithium-ion battery energy storage system to achieve renewable power dispatchability," *Appl. Energy*, vol. 260, p. 114,282, Feb. 2020. doi: 10.1016/j.apenergy.2019.114282.
- [8] S. Xie, X. Hu, Q. Zhang, X. Lin, B. Mu, and H. Ji, "Aging-aware co-optimization of battery size, depth of discharge, and energy management for plug-in hybrid electric vehicles," *J. Power Sources*, vol. 450, p. 227,638, Feb. 2020. doi: 10.1016/j.jpowsour.2019.227638.
- [9] X. Hu, K. Zhang, K. Liu, X. Lin, S. Dey, and S. Onori, "Advanced fault diagnosis for lithium-ion battery systems: A review of fault mechanisms, fault features, and diagnosis procedures," *IEEE Ind. Electron. Mag.*, vol. 14, no. 3, pp. 65–91, Sept. 2020. doi: 10.1109/MIE.2020.2964814.
- [10] R. Gu, P. Malysz, H. Yang, and A. Emadi, "On the suitability of electrochemical-based modeling for lithium-ion batteries," *IEEE Trans. Transport. Electrific.*, vol. 2, no. 4, pp. 417–431, Dec. 2016. doi: 10.1109/TTE.2016.2571778.
- [11] U. Krewer, F. Röder, E. Harinath, R. D. Braatz, B. Bedürftig, and R. Findeisen, "Dynamic models of Li-ion batteries for diagnosis and operation: A review and perspective," *J. Electrochem. Soc.*, vol. 165, no. 16, pp. A3656–A3673, Jan. 2018. doi: 10.1149/2.1061814jes.
- [12] M. T. Lawder et al., "Battery energy storage system (BESS) and battery management system (BMS) for grid-scale applications," *Proc. IEEE*, vol. 102, no. 6, pp. 1014–1030, June 2014. doi: 10.1109/JPROC.2014.2317451.
- [13] A. Seaman, T.-S. Dao, and J. McPhee, "A survey of mathematics-based equivalent-circuit and electrochemical battery models for hybrid and electric vehicle simulation," *J. Power Sources*, vol. 256, pp. 410–423, July 2014. doi: 10.1016/j.jpowsour.2014.01.057.
- [14] N. A. Chaturvedi, R. Klein, J. Christensen, J. Ahmed, and A. Kojic, "Algorithms for advanced battery-management systems," *IEEE Control Syst. Mag.*, vol. 30, no. 3, pp. 49–68, June 2010.

- [15] S. Kolluri, S. V. Aduru, M. Pathak, R. D. Braatz, and V. R. Subramanian, "Real-time nonlinear model predictive control (NMPC) strategies using physics-based models for advanced lithium-ion battery management system (BMS)," *J. Electrochem. Soc.*, vol. 167, no. 6, p. 063505, Apr. 2020. doi: 10.1149/1945-7111/ab7bd7.
- [16] M. Doyle, T. F. Fuller, and J. Newman, "Modeling of galvanostatic charge and discharge of the lithium/polymer/insertion cell," *J. Electrochem. Soc.*, vol. 140, no. 6, pp. 1526–1533, Jan. 1993. doi: 10.1149/1.2221597.
- [17] T. F. Fuller, M. Doyle, and J. Newman, "Simulation and optimization of the dual lithium ion insertion cell," *J. Electrochem. Soc.*, vol. 141, no. 1, pp. 1–10, 1994. doi: 10.1149/1.2054684.
- [18] M. Doyle and J. Newman, "Modeling the performance of rechargeable lithium-based cells: Design correlations for limiting cases," *J. Power Sources*, vol. 54, no. 1, pp. 46–51, Mar. 1995. doi: 10.1016/0378-7753(94)02038-5.
- [19] Y. Li, M. Vilathgamuwa, T. Farrell, S. S. Choi, N. T. Tran, and J. Teague, "A physics-based distributed-parameter equivalent circuit model for lithium-ion batteries," *Electrochim. Acta*, vol. 299, pp. 451–469, Mar. 2019. doi: 10.1016/j.electacta.2018.12.167.
- [20] M. Torchio, L. Magni, R. B. Gopaluni, R. D. Braatz, and D. M. Raimondo, "LIONSIMBA: A Matlab framework based on a finite volume model suitable for Li-ion battery design, simulation, and control," *J. Electrochem. Soc.*, vol. 163, no. 7, pp. A1192–A1205, Jan. 2016. doi: 10.1149/2.0291607jes.
- [21] V. R. Subramanian, V. Boovaragavan, V. Ramadesigan, and M. Arabandi, "Mathematical model reformulation for lithium-ion battery simulations: Galvanostatic boundary conditions," *J. Electrochem. Soc.*, vol. 156, no. 4, pp. A260–A271, Apr. 2009. doi: 10.1149/1.3065083.
- [22] M. Safari and C. Delacourt, "Modeling of a commercial graphite/LiFePO₄ cell," *J. Electrochem. Soc.*, vol. 158, no. 5, pp. A562–A571, May 2011. doi: 10.1149/1.3567007.
- [23] M. Guo and R. E. White, "A distributed thermal model for a Li-ion electrode plate pair," *J. Power Sources*, vol. 221, pp. 334–344, Jan. 2013. doi: 10.1016/j.jpowsour.2012.08.012.
- [24] J. Sturm et al., "Suitability of physicochemical models for embedded systems regarding a nickel-rich, silicon-graphite lithium-ion battery," *J. Power Sources*, vol. 436, pp. 226,834, Oct. 2019. doi: 10.1016/j.jpowsour.2019.226834.
- [25] J. M. Reniers, G. Mulder, and D. A. Howey, "Review and performance comparison of mechanical-chemical degradation models for lithium-ion batteries," *J. Electrochem. Soc.*, vol. 166, no. 14, pp. A3189–A3200, Sept. 2019. doi: 10.1149/2.0281914jes.
- [26] B. Wu, W. D. Widanage, S. Yang, and X. Liu, "Battery digital twins: Perspectives on the fusion of models, data and artificial intelligence for smart battery management systems," *Energy AI*, vol. 1, p. 100,016, Aug. 2020. doi: 10.1016/j.egyai.2020.100016.
- [27] K. A. Smith, C. D. Rahn, and C.-Y. Wang, "Control oriented 1D electrochemical model of lithium ion battery," *Energy Convers. Manag.*, vol. 48, no. 9, pp. 2565–2578, Sept. 2007. doi: 10.1016/j.enconman.2007.03.015.
- [28] A. Allam and S. Onori, "Online capacity estimation for lithium-ion battery cells via an electrochemical model-based adaptive interconnected observer," *IEEE Trans. Control Syst. Technol.*, vol. 29, no. 4, pp. 1636–1651, July 2021. doi: 10.1109/TCST.2020.3017566.
- [29] L. Zheng, J. Zhu, G. Wang, D. D. Lu, and T. He, "Lithium-ion battery instantaneous available power prediction using surface lithium concentration of solid particles in a simplified electrochemical model," *IEEE Trans. Power Electron.*, vol. 33, no. 11, pp. 9551–9560, Nov. 2018. doi: 10.1109/TPEL.2018.2791965.
- [30] Z. T. Gima, D. Kato, R. Klein, and S. J. Moura, "Analysis of online parameter estimation for electrochemical Li-ion battery models via reduced sensitivity equations," in *Proc. Amer. Control Conf.*, Denver, CO, July 1–3, 2020, pp. 373–378.
- [31] A. Pozzi, M. Zambelli, A. Ferrara, and D. M. Raimondo, "Balancing-aware charging strategy for series-connected lithium-ion cells: A nonlinear model predictive control approach," *IEEE Trans. Control Syst. Technol.*, vol. 28, no. 5, pp. 1862–1877, Sept. 2020. doi: 10.1109/TCST.2020.2995308.
- [32] M. A. Rahman, S. Anwar, and A. Izadian, "Electrochemical model based fault diagnosis of a lithium ion battery using multiple model adaptive estimation approach," in *Proc. IEEE Int. Conf. Ind. Technol.*, Seville, Spain, Mar. 17–19, 2015, pp. 210–217.
- [33] C. Zou, X. Hu, Z. Wei, T. Wik, and B. Egardt, "Electrochemical estimation and control for lithium-ion battery health-aware fast charging," *IEEE Trans. Ind. Electron.*, vol. 65, no. 8, pp. 6635–6645, Aug. 2018. doi: 10.1109/TIE.2017.2772154.
- [34] M.-T. von Sbrik, M. Marinescu, R. F. Martinez-Botas, and G. J. Offer, "A physically meaningful equivalent circuit network model of a lithium-ion battery accounting for local electrochemical and thermal behaviour, variable double layer capacitance and degradation," *J. Power Sources*, vol. 325, pp. 171–184, Sept. 2016. doi: 10.1016/j.jpowsour.2016.05.051.
- [35] Y. Merla, B. Wu, V. Yufit, R. F. Martinez-Botas, and G. J. Offer, "An easy-to-parameterise physics-informed battery model and its application towards lithium-ion battery cell design, diagnosis, and degradation," *J. Power Sources*, vol. 384, pp. 66–79, Apr. 2018. doi: 10.1016/j.jpowsour.2018.02.065.
- [36] M. Corno, "Efficient control-oriented coupled electrochemical thermal modeling of Li-ion cells," *IEEE Trans. Ind. Electron.*, vol. 68, no. 8, pp. 7024–7033, Aug. 2021. doi: 10.1109/TIE.2020.3008377.
- [37] J. Sturm, H. Ennifar, S. V. Erhard, A. Rheinfeld, S. Kosch, and A. Jossen, "State estimation of lithium-ion cells using a physicochemical model based extended Kalman filter," *Appl. Energy*, vol. 223, pp. 103–123, Aug. 2018. doi: 10.1016/j.apenergy.2018.04.011.
- [38] D. D. Domenico, A. Stefanopoulou, and G. Fiengo, "Lithium-ion battery state of charge and critical surface charge estimation using an electrochemical model-based extended Kalman filter," *J. Dynamic Syst. Meas. Control*, vol. 132, no. 6, p. 061302, Nov. 2010.
- [39] L. Cai and R. E. White, "Reduction of model order based on proper orthogonal decomposition for lithium-ion battery simulations," *J. Electrochem. Soc.*, vol. 156, no. 3, pp. A154–A161, Mar. 2009. doi: 10.1149/1.3049347.
- [40] Y. Zeng et al., "Efficient conservative numerical schemes for 1D nonlinear spherical diffusion equations with applications in battery modeling," *J. Electrochem. Soc.*, vol. 160, no. 9, pp. A1565–A1571, Jan. 2013. doi: 10.1149/2.102309jes.
- [41] D. Zhang, S. Dey, L. D. Couto, and S. J. Moura, "Battery adaptive observer for a single-particle model with intercalation-induced stress," *IEEE Trans. Control Syst. Technol.*, vol. 28, no. 4, pp. 1363–1377, July 2020. doi: 10.1109/TCST.2019.2910797.
- [42] R. Achar and M. S. Nakhla, "Simulation of high-speed interconnects," *Proc. IEEE*, vol. 89, no. 5, pp. 693–728, May 2001. doi: 10.1109/5.929650.
- [43] W. He, M. Pecht, D. Flynn, and F. Dinmohammadi, "A physics-based electrochemical model for lithium-ion battery state-of-charge estimation solved by an optimised projection-based method and moving-win-
- dow-filtering," *Energies*, vol. 11, no. 8, p. 2120, 2018. doi: 10.3390/en11082120.
- [44] T.-S. Dao, C. P. Vyasarayani, and J. McPhee, "Simplification and order reduction of lithium-ion battery model based on porous-electrode theory," *J. Power Sources*, vol. 198, pp. 329–337, Jan. 2012. doi: 10.1016/j.jpowsour.2011.09.034.
- [45] A. M. Bizeray, S. Zhao, S. R. Duncan, and D. A. Howey, "Lithium-ion battery thermal-electrochemical model-based state estimation using orthogonal collocation and a modified extended Kalman filter," *J. Power Sources*, vol. 296, pp. 400–412, Nov. 2015. doi: 10.1016/j.jpowsour.2015.07.019.
- [46] D. W. Limoge, P. Y. Bi, A. M. Annaswamy, and A. Krupadanam, "A reduced-order model of a lithium-ion cell using the absolute nodal coordinate formulation approach," *IEEE Trans. Control Syst. Technol.*, vol. 26, no. 3, pp. 1001–1014, May 2018. doi: 10.1109/TCST.2017.2692743.
- [47] G. Fan, X. Li, and M. Canova, "A reduced-order electrochemical model of Li-ion batteries for control and estimation applications," *IEEE Trans. Veh. Technol.*, vol. 67, no. 1, pp. 76–91, Jan. 2018. doi: 10.1109/TVT.2017.2738780.
- [48] L. Cai and R. E. White, "Lithium-ion cell modeling using orthogonal collocation on finite elements," *J. Power Sources*, vol. 217, pp. 248–255, Nov. 2012. doi: 10.1016/j.jpowsour.2012.06.043.
- [49] J. Liu, G. Li, and H. K. Fathy, "An extended differential flatness approach for the health-conscious nonlinear model predictive control of lithium-ion batteries," *IEEE Trans. Control Syst. Technol.*, vol. 25, no. 5, pp. 1882–1889, Sept. 2017. doi: 10.1109/TCST.2016.2624143.
- [50] V. R. Subramanian, V. D. Diwakar, and D. Tapriyal, "Efficient macro-micro scale coupled modeling of batteries," *J. Electrochem. Soc.*, vol. 152, no. 10, pp. A2002–A2008, Aug. 2005. doi: 10.1149/1.2032427.
- [51] S. Santhanagopalan, Q. Guo, P. Ramadass, and R. E. White, "Review of models for predicting the cycling performance of lithium-ion batteries," *J. Power Sources*, vol. 156, no. 2, pp. 620–628, June 2006. doi: 10.1016/j.jpowsour.2005.05.070.
- [52] Y. Li et al., "Electrochemical model-based fast charging: Physical constraint-triggered PI control," *IEEE Trans. Energy Convers.*, early access. doi: 10.1109/TEC.2021.3065983.
- [53] K. A. Smith, C. D. Rahn, and C.-Y. Wang, "Model-based electrochemical estimation and constraint management for pulse operation of lithium ion batteries," *IEEE Trans. Control Syst. Technol.*, vol. 18, no. 3, pp. 654–663, May 2010. doi: 10.1109/TCST.2009.2027023.
- [54] H. Zhao, M. Hong, W. Lin, and K. A. Loparo, "Voltage and frequency regulation of microgrid with battery energy storage systems," *IEEE Trans. Smart Grid*, vol. 10, no. 1, pp. 414–424, Jan. 2019. doi: 10.1109/TSG.2017.2741668.
- [55] S. Khaleghi Rahimian, S. Rayman, and R. E. White, "Extension of physics-based single particle model for higher charge-discharge rates," *J. Power Sources*, vol. 224, pp. 180–194, Feb. 2013. doi: 10.1016/j.jpowsour.2012.09.084.
- [56] M. Guo and R. E. White, "An approximate solution for solid-phase diffusion in a spherical particle in physics-based Li-ion cell models," *J. Power Sources*, vol. 198, pp. 322–328, Jan. 2012. doi: 10.1016/j.jpowsour.2011.08.096.
- [57] N. T. Tran, M. Vilathgamuwa, T. Farrell, S. S. Choi, Y. Li, and J. Teague, "A Padé approximate model of lithium ion batteries," *J. Electrochem. Soc.*, vol. 165, no. 7, pp. A1409–A1421, May 2018. doi: 10.1149/2.0651807jes.
- [58] N. T. Tran, M. Vilathgamuwa, T. Farrell, S. S. Choi, and Y. Li, "A computationally efficient coupled electrochemical-thermal

- model for large format cylindrical lithium ion batteries," *J. Electrochem. Soc.*, vol. 166, no. 13, pp. A3059–A3071, Sept. 2019. doi: 10.1149/2.1241913jes.
- [59] J. L. Lee, A. Chemstruck, and G. L. Plett, "One-dimensional physics-based reduced-order model of lithium-ion dynamics," *J. Power Sources*, vol. 220, pp. 430–448, Dec. 2012. doi: 10.1016/j.jpowsour.2012.07.075.
- [60] A. Rodríguez, G. L. Plett, and M. S. Trimboli, "Comparing four model-order reduction techniques, applied to lithium-ion battery-cell internal electrochemical transfer functions," *eTransport*, vol. 1, p. 100,009, Aug. 2019. doi: 10.1016/j.etrans.2019.100009.
- [61] A. Rodríguez, G. L. Plett, and M. S. Trimboli, "Improved transfer functions modeling linearized lithium-ion battery-cell internal electrochemical variables," *J. Energy Storage*, vol. 20, pp. 560–575, Dec. 2018. doi: 10.1016/j.est.2018.06.015.
- [62] Y. Li, M. Vilathgamuwa, S. S. Choi, T. W. Farrell, N. T. Tran, and J. Teague, "Development of a degradation-conscious physics-based lithium-ion battery model for use in power system planning studies," *Appl. Energy*, vol. 248, pp. 512–525, Aug. 2019. doi: 10.1016/j.apenergy.2019.04.143.
- [63] J. M. Reniers, G. Mulder, and D. A. Howey, "Unlocking extra value from grid batteries using advanced models," *J. Power Sources*, vol. 487, p. 229,355, Mar. 2021. doi: 10.1016/j.jpowsour.2020.229355.
- [64] R. Klein, N. A. Chaturvedi, J. Christensen, J. Ahmed, R. Findeisen, and A. Kojic, "Electrochemical model-based observer design for a lithium-ion battery," *IEEE Trans. Control Syst. Technol.*, vol. 21, no. 2, pp. 289–301, Jan. 2011. doi: 10.1109/TCST.2011.2178604.
- [65] J. Marcicki, M. Canova, A. T. Conlisk, and G. Rizzoni, "Design and parametrization analysis of a reduced-order electrochemical model of graphite/LiFePO₄ cells for SOC/SOH estimation," *J. Power Sources*, vol. 237, pp. 310–324, Sept. 2013. doi: 10.1016/j.jpowsour.2012.12.120.
- [66] S. J. Moura, F. B. Argomedo, R. Klein, A. Mirtabatabaei, and M. Krstic, "Battery state estimation for a single particle model with electrolyte dynamics," *IEEE Trans. Control Syst. Technol.*, vol. 25, no. 2, pp. 453–468, Mar. 2017. doi: 10.1109/TCST.2016.2571663.
- [67] J. Newman, "Fortran programs for the simulation of electrochemical systems." [Online]. Available: <http://www.cchem.berkeley.edu/jsngrp/fortran.html> (accessed 30 July 2021)
- [68] S. Moura, "FastDFN: Fast Doyle-Fuller-Newman (DFN) electrochemical-thermal battery model simulator," GitHub, San Francisco, 2018. [Online]. Available: <https://github.com/scott-moura/fastDFN>
- [69] V. Sulzer, S. G. Marquis, R. Timms, M. Robinson, and S. J. Chapman, "Python battery mathematical modelling (PyBaMM)," *J. Open Res. Softw.*, vol. 9, no. 1, p. 14, Jun. [Online]. Available: <https://github.com/pybamm-team/PyBaMM>
- [70] S. Dey, B. Ayalew, and P. Pisu, "Nonlinear robust observers for state-of-charge estimation of lithium-ion cells based on a reduced electrochemical model," *IEEE Trans. Control Syst. Technol.*, vol. 23, no. 5, pp. 1935–1942, Sept. 2015. doi: 10.1109/TCST.2014.2382635.
- [71] S. Marelli and M. Corno, "Model-based estimation of lithium concentrations and temperature in batteries using soft-constrained dual unscented Kalman filtering," *IEEE Trans. Control Syst. Technol.*, vol. 29, no. 2, pp. 926–933, Mar. 2021. doi: 10.1109/TCST.2020.2974176.
- [72] W. Li et al., "Electrochemical model-based state estimation for lithium-ion batteries with adaptive unscented Kalman filter," *J. Power Sources*, vol. 476, p. 228,534, Nov. 2020. doi: 10.1016/j.jpowsour.2020.228534.
- [73] R. Ahmed, M. E. Sayed, I. Arasaratnam, J. Tjong, and S. Habibi, "Reduced-order electrochemical model parameters identification and SOC estimation for healthy and aged Li-ion batteries Part I: Parameterization model development for healthy batteries," *IEEE J. Emerg. Sel. Topics Power Electron.*, vol. 2, no. 3, pp. 659–677, Sept. 2014. doi: 10.1109/JESTPE.2014.2331059.
- [74] H. Perez, N. Shahmohammadhamedani, and S. Moura, "Enhanced performance of Li-ion batteries via modified reference governors and electrochemical models," *IEEE/ASME Trans. Mechatron.*, vol. 20, no. 4, pp. 1511–1520, Aug. 2015. doi: 10.1109/TMECH.2014.2379695.
- [75] C. Zou, C. Manzie, and D. Nešić, "Model predictive control for lithium-ion battery optimal charging," *IEEE/ASME Trans. Mechatron.*, vol. 23, no. 2, pp. 947–957, Apr. 2018. doi: 10.1109/TMECH.2018.2798930.
- [76] Y. Li, B. Xiong, D. M. Vilathgamuwa, Z. Wei, C. Xie, and C. Zou, "Constrained ensemble Kalman filter for distributed electrochemical state estimation of lithium-ion batteries," *IEEE Trans. Ind. Inform.*, vol. 17, no. 1, pp. 240–250, Jan. 2021. doi: 10.1109/TII.2020.2974907.
- [77] T. R. Ashwin, A. McGordon, W. D. Widanage, and P. A. Jennings, "Modified electrochemical parameter estimation of NCR18650BD battery using implicit finite volume method," *J. Power Sources*, vol. 341, pp. 387–395, Feb. 2017. doi: 10.1016/j.jpowsour.2016.12.023.
- [78] A. Pozzi, M. Torchio, R. D. Braatz, and D. M. Raimondo, "Optimal charging of an electric vehicle battery pack: A real-time sensitivity-based model predictive control approach," *J. Power Sources*, vol. 461, p. 228,133, June 2020. doi: 10.1016/j.jpowsour.2020.228133.
- [79] M. Torchio, L. Magni, R. D. Braatz, and D. M. Raimondo, "Optimal health-aware charging protocol for lithium-ion batteries: A fast model predictive control approach," *IFAC PapersOnLine*, vol. 49, no. 7, pp. 827–832, Jan. 2016. doi: 10.1016/j.ifacol.2016.07.292.
- [80] V. Ramadesigan, K. Chen, N. A. Burns, V. Boovaragavan, R. D. Braatz, and V. R. Subramanian, "Parameter estimation and capacity fade analysis of lithium-ion batteries using reformulated models," *J. Electrochem. Soc.*, vol. 158, no. 9, p. A1048, July 2011. doi: 10.1149/1.3609926.
- [81] D. W. Limoge and A. M. Annaswamy, "An adaptive observer design for real-time parameter estimation in lithium-ion batteries," *IEEE Trans. Control Syst. Technol.*, vol. 28, no. 2, pp. 505–520, Mar. 2020. doi: 10.1109/TCST.2018.2885962.
- [82] M. S. S. Malik, G. Li, and Z. Chen, "An optimal charging algorithm to minimise solid electrolyte interface layer in lithium-ion battery," *J. Power Sources*, vol. 482, p. 228,895, Jan. 2021. doi: 10.1016/j.jpowsour.2020.228895.
- [83] H. E. Perez, S. Dey, X. Hu, and S. J. Moura, "Optimal charging of Li-ion batteries via a single particle model with electrolyte and thermal dynamics," *J. Electrochem. Soc.*, vol. 164, no. 7, pp. A1679–A1687, June 2017. doi: 10.1149/2.1301707jes.
- [84] N. Lotfi, R. G. Landers, J. Li, and J. Park, "Reduced-order electrochemical model-based SOC observer with output model uncertainty estimation," *IEEE Trans. Control Syst. Technol.*, vol. 25, no. 4, pp. 1217–1230, July 2017. doi: 10.1109/TCST.2016.2598764.
- [85] X. Hu, D. Cao, and B. Egardt, "Condition monitoring in advanced battery management systems: Moving horizon estimation using a reduced electrochemical model," *IEEE/ASME Trans. Mechatron.*, vol. 23, no. 1, pp. 167–178, Feb. 2018. doi: 10.1109/TMECH.2017.2675920.
- [86] B. Jenkins, A. Krupadanam, and A. M. Annaswamy, "Fast adaptive observers for battery management systems," *IEEE Trans. Control Syst. Technol.*, vol. 28, no. 3, pp. 776–789, May 2020. doi: 10.1109/TCST.2019.2891234.
- [87] M. K. S. Verma et al., "On-board state estimation in electrical vehicles: Achieving accuracy and computational efficiency through an electrochemical model," *IEEE Trans. Veh. Technol.*, vol. 69, no. 3, pp. 2563–2575, Mar. 2020. doi: 10.1109/TVT.2020.2966266.
- [88] B. Liu, X. Tang, and F. Gao, "Joint estimation of battery state-of-charge and state-of-health based on a simplified pseudo-two-dimensional model," *Electrochim. Acta*, vol. 344, p. 136,098, June 2020. doi: 10.1016/j.electacta.2020.136098.
- [89] Y. Liu et al., "A nonlinear observer SOC estimation method based on electrochemical model for lithium-ion battery," *IEEE Trans. Ind. Appl.*, vol. 57, no. 1, pp. 1094–1104, Jan./Feb. 2021. doi: 10.1109/TIA.2020.3040140.
- [90] Y. Yin, Y. Hu, S.-Y. Choe, H. Cho, and W. T. Joe, "New fast charging method of lithium-ion batteries based on a reduced order electrochemical model considering side reaction," *J. Power Sources*, vol. 423, pp. 367–379, May 2019. doi: 10.1016/j.jpowsour.2019.03.007.
- [91] Y. Bi, Y. Yin, and S.-Y. Choe, "Online state of health and aging parameter estimation using a physics-based life model with a particle filter," *J. Power Sources*, vol. 476, pp. 228655, Nov. 2020. doi: 10.1016/j.jpowsour.2020.228655.
- [92] Y. Yin and S.-Y. Choe, "Actively temperature controlled health-aware fast charging method for lithium-ion battery using nonlinear model predictive control," *Appl. Energy*, vol. 271, p. 115232, Aug. 2020. doi: 10.1016/j.apenergy.2020.115232.
- [93] M. Song and S.-Y. Choe, "Fast and safe charging method suppressing side reaction and lithium deposition reaction in lithium ion battery," *J. Power Sources*, vol. 436, p. 226,835, Oct. 2019. doi: 10.1016/j.jpowsour.2019.226835.
- [94] A. Bartlett, J. Marcicki, S. Onori, G. Rizzoni, X. G. Yang, and T. Miller, "Electrochemical model-based state of charge and capacity estimation for a composite electrode lithium-ion battery," *IEEE Trans. Control Syst. Technol.*, vol. 24, no. 2, pp. 384–399, Mar. 2016.
- [95] X. Zhang, J. Lu, S. Yuan, J. Yang, and X. Zhou, "A novel method for identification of lithium-ion battery equivalent circuit model parameters considering electrochemical properties," *J. Power Sources*, vol. 345, pp. 21–29, Mar. 2017. doi: 10.1016/j.jpowsour.2017.01.126.
- [96] Y. Gao et al., "Health-aware multiobjective optimal charging strategy with coupled electrochemical-thermal-aging model for lithium-ion battery," *IEEE Trans. Ind. Inform.*, vol. 16, no. 5, pp. 3417–3429, May 2020. doi: 10.1109/TII.2019.2935326.
- [97] S. Park, D. Lee, H. J. Ahn, C. Tomlin, and S. Moura, "Optimal control of battery fast charging based-on Pontryagin's minimum principle," in *Proc. IEEE Conf. Decis. Control*, Jeju, South Korea, Dec. 14–18, 2020, pp. 3506–3513.
- [98] L. De Pascali, F. Biral, and S. Onori, "Aging-aware optimal energy management control for a parallel hybrid vehicle based on electrochemical-degradation dynamics," *IEEE Trans. Veh. Technol.*, vol. 69, no. 10, pp. 10,868–10,878, Oct. 2020. doi: 10.1109/TVT.2020.3019241.
- [99] K. D. Stetzel, L. L. Aldrich, M. S. Trimboli, and G. L. Plett, "Electrochemical state and internal variables estimation using a reduced-order physics-based model of a lithium-ion cell and an extended Kalman filter," *J. Power Sources*, vol. 278, pp. 490–505, Mar. 2015. doi: 10.1016/j.jpowsour.2014.11.135.
- [100] M. A. Xavier, A. K. d. Souza, K. Karami, G. L. Plett, and M. S. Trimboli, "A computational framework for lithium-ion cell-level model

- predictive control using a physics-based reduced-order model," *IEEE Control Syst. Lett.*, vol. 5, no. 4, pp. 1387–1392, Oct. 2021. doi: 10.1109/LCSYS.2020.3038131.
- [101] S. K. Rahimian, S. Rayman, and R. E. White, "State of charge and loss of active material estimation of a lithium-ion cell under low earth orbit condition using Kalman filtering approaches," *J. Electrochem. Soc.*, vol. 159, no. 6, pp. A860–A872, Jan. 2012. doi: 10.1149/2.098206jes.
- [102] R. Ahmed, M. E. Sayed, I. Arasaratnam, J. Tjong, and S. Habibi, "Reduced-order electrochemical model parameters identification and state of charge estimation for healthy and aged Li-ion batteries—Part II: Aged battery model and state of charge estimation," *IEEE J. Emerg. Sel. Topics Power Electron.*, vol. 2, no. 3, pp. 678–690, Sept. 2014. doi: 10.1109/JESTPE.2014.2331062.
- [103] S. J. Moura, N. A. Chaturvedi, and M. Krstic, "Adaptive partial differential equation observer for battery state-of-charge/state-of-health estimation via an electrochemical model," *J. Dyn. Syst. Meas. Control*, vol. 136, no. 1, p. 11015, Jan. 2014.
- [104] X. Lin, X. Hao, Z. Liu, and W. Jia, "Health conscious fast charging of Li-ion batteries via a single particle model with aging mechanisms," *J. Power Sources*, vol. 400, pp. 305–316, Oct. 2018. doi: 10.1016/j.jpowsour.2018.08.030.
- [105] F. Lam, A. Allam, W. T. Joe, Y. Choi, and S. Onori, "Offline multiobjective optimization for fast charging and reduced degradation in lithium-ion battery cells using electrochemical dynamics," *IEEE Control Syst. Lett.*, vol. 5, no. 6, pp. 2066–2071, Dec. 2021. doi: 10.1109/LCSYS.2020.3046378.
- [106] F. Feng, X. Hu, L. Hu, F. Hu, Y. Li, and L. Zhang, "Propagation mechanisms and diagnosis of parameter inconsistency within Li-ion battery packs," *Renew. Sustain. Energy Rev.*, vol. 112, pp. 102–113, Sept. 2019. doi: 10.1016/j.rser.2019.05.042.
- [107] W. Han, T. Wik, A. Kersten, G. Dong, and C. Zou, "Next-generation battery management systems: Dynamic reconfiguration," *IEEE Ind. Electron. Mag.*, vol. 14, no. 4, pp. 20–31, Dec. 2020. doi: 10.1109/MIE.2020.3002486.
- [108] K. A. Severson et al., "Data-driven prediction of battery cycle life before capacity degradation," *Nature Energy*, vol. 4, no. 5, pp. 383–391, May 2019. doi: 10.1038/s41560-019-0356-8.
- [109] Y. Tan and G. Zhao, "Transfer learning with long short-term memory network for state-of-health prediction of lithium-ion batteries," *IEEE Trans. Ind. Electron.*, vol. 67, no. 10, pp. 8723–8731, Oct. 2020. doi: 10.1109/TIE.2019.2946551.
- [110] X. Tang, C. Zou, K. Yao, J. Lu, Y. Xia, and F. Gao, "Aging trajectory prediction for lithium-ion batteries via model migration and Bayesian Monte Carlo method," *Appl. Energy*, vol. 254, p. 113591, Nov. 2019. doi: 10.1016/j.apenergy.2019.113591.
- [111] J. Wei, G. Dong, and Z. Chen, "Remaining useful life prediction and state of health diagnosis for lithium-ion batteries using particle filter and support vector regression," *IEEE Trans. Ind. Electron.*, vol. 65, no. 7, pp. 5634–5643, July 2018. doi: 10.1109/TIE.2017.2782224.
- [112] M. Aykol et al., "Perspective—Combining physics and machine learning to predict battery lifetime," *J. Electrochem. Soc.*, vol. 168, no. 3, p. 30525, Mar. 2021. doi: 10.1149/1945-7111/abec55.
- [113] Z. Wei, J. Zhao, H. He, G. Ding, H. Cui, and L. Liu, "Future smart battery and management: Advanced sensing from external to embedded multi-dimensional measurement," *J. Power Sources*, vol. 489, p. 229462, Mar. 2021. doi: 10.1016/j.jpowsour.2021.229462.
- [114] A. M. Bizeray, J. Kim, S. R. Duncan, and D. A. Howey, "Identifiability and parameter estimation of the single particle lithium-ion battery model," *IEEE Trans. Control Syst. Technol.*, vol. 27, no. 5, pp. 1862–1877, Sept. 2019. doi: 10.1109/TCST.2018.2838097.
- [115] Z. Chu, R. Jobman, A. Rodriguez, G. L. Plett, M. S. Trimboli, X. Feng, et al. "A control-oriented electrochemical model for lithium-ion battery. Part II: Parameter identification based on reference electrode," *J. Energy Storage*, vol. 27, p. 101101, Feb. 2020. doi: 10.1016/j.est.2019.101101.

